CAMS Service Evolution

D7.2 Report on the importance of biogenic aerosols

Due date of deliverable	30/6/2025
Submission date	4/7/2025
File Name	
Work Package /Task	WP7, Task 7.3, Report on the importance of biogenic aerosols
Organisation Responsible of Deliverable	METNorway
Author name(s)	Samuel Remy, Gunnar Lange
Revision number	1.0
Status	
Dissemination Level	PU

Funded by the European Union

The CAMAERA project (grant agreement No 101134927) is funded by the European Union.
Views and opinions expressed are however those of the author(s) only and do not necessarily reflect those of the European Union or the Commission. Neither the European Union nor the granting authority can be held responsible for them.

1 Executive Summary

Fungal spores are less well known allergens than pollens. However, they still represent a major public health issue, and, because of their smaller size, they can contribute a significant fraction of PM10, a key CAMS products. This is why the test implementation of a fungal spores species in a regional and the global CAMS systems has been pursued in this deliverable. Several emission schemes has been tested and inter-compared, and the resulting simulations of fungal spores surface concentration have been evaluated and inter-compared, also with data from the CHIMERE model. A significant part of the work concerned finding observational data for evaluation, as fungal spores data are sparse and in general not public. Two key datasets have been retrieved and processed for evaluation, over Europe and U.S. The impact on simulated PM10 has also been assessed. The main characteristics of the fungal spores implementation in EMEP and IFS-COMPO can be summarized as such:

- Fungal spores represent a significant fraction of simulated PM10 over Europe in summertime (10-20%) and over tropical and equatorial forests all year long,
- The emission schemes tested are able to represent the seasonal cycle of fungal spores quite accurately, except over some locations, and for some features (autumn emissions peak)
- The correlation between daily or three daily simulated and observed surface concentration of a fungal spores proxy is quite satisfactory
- Some uncertainty exists on the key LAI input which can have a large impact on simulated fungal spores emissions

Table of Contents

2 Introduction

2.1 Background

The European Union's flagship Space programme Copernicus provides a key service to the European society, turning investments in space-infrastructure into high-quality information products. The Copernicus Atmosphere Monitoring Service (CAMS, https://atmosphere.copernicus.eu) exploits the information content of Earth-Observation data to monitor the composition of the atmosphere. By combining satellite observations with numerical modelling by means of data assimilation and inversion techniques, CAMS provides in near-real time a wealth of information to answer questions related to air quality, climate change and air pollution and its mitigation, energy, agriculture, etc. CAMS provides both global atmospheric composition products, using the Integrated Forecasting System (IFS) of ECMWF - hereafter denoted the global production system -, and regional European products, provided by an ensemble of eleven regional models - the regional production system.

The CAMS AERosol Advancement (CAMAERA) project will provide strong improvements of the aerosol modelling capabilities of the regional and global systems, on the assimilation of new sources of data, and on a better representation of secondary aerosols and their precursor gases. In this way CAMAERA will enhance the quality of key products of the CAMS service and therefore help CAMS to better respond to user needs such as air pollutant monitoring, along with the fulfilment of sustainable development goals. To achieve this purpose CAMAERA will develop new prototype service elements of CAMS, beyond the current state-of-art. It will do so in very close collaboration with the CAMS service providers, as well as other tier-3 projects. In particular CAMAERA will complement research topics addressed in CAMEO, which focuses on the preparation for novel satellite data, improvements of the data assimilation and inversion capabilities of the CAMS production system, and the provision of uncertainty information of CAMS products.

2.2 Scope of this deliverable

2.2.1 Objectives of this deliverables

This deliverable documents the implementation of a lumped fungal spores species in the EMEP and IFS-COMPO systems (global CAMS system), the evaluation of the simulated surface concentration as well as the impact on PM10 and others.

2.2.2 Work performed in this deliverable

In this deliverable the work as planned in the Description of Action (DoA, WP7 T7.3) was performed.

2.2.3 Deviations and counter measures

This deliverable focused on fungal spores, and not on other bioaersols such as pollen and bacteria. We preferred to avoid resource dispersion and focus our efforts on implementing several schemes for fungal spores in both regional (EMEP) and global (IFS-COMPO) CAMS systems.

2.2.4 CAMAERA Project Partners:

HYGEOS	HYGEOS SARL
ECMWF	EUROPEAN CENTRE FOR MEDIUM-RANGE WEATHER FORECASTS
Met Norway	METEOROLOGISK INSTITUTT
RC.io	RESEARCHCONCEPTS IO
BSC	BARCELONA SUPERCOMPUTING CENTER-CENTRO NACIONAL DE SUPERCOMPUTACION
KNMI	KONINKLIJK NEDERLANDS METEOROLOGISCH INSTITUUT-KNMi
SMHI	SVERIGES METEOROLOGISKA OCH HYDROLOGISKA INSTITUT
FMI	ILMATIETEEN LAITOS
MF	METEO-FRANCE
TNO	NEDERLANDSE ORGANISATIE VOOR TOEGEPAST NATUURWETENSCHAPPELIJK ONDERZOEK TNO
INERIS	INSTITUT NATIONAL DE L ENVIRONNEMENT INDUSTRIEL ET DES RISQUES - INERIS
IOS-PIB	INSTYTUT OCHRONY SRODOWISKA - PANSTWOWY INSTYTUT BADAWCZY
FZJ	FORSCHUNGSZENTRUM JULICH GMBH
AU	AARHUS UNIVERSITET
ENEA	AGENZIA NAZIONALE PER LE NUOVE TECNOLOGIE, L'ENERGIA E LO SVILUPPO ECONOMICO SOSTENIBILE

3 Bioaerosols: why do they matter?

Primary Biological Aerosol Particles (PBAPs), commonly known also as bioaerosols, are airborne particles that include mainly bacteria, fungi spores, pollen, viruses, microorganisms or even leaf debris and usually dominate the aerosol mass over remote forested regions. Bioaerosols are omnipresent in the global atmosphere; they can be alive, dead, dormant like bacteria, viruses and fungi spores, or can be released from leaving organisms like pollen, cell debris and biofilms. Their sizes vary from less than 0.3 µm for viruses to about 100 µm for pollens (Després et al., 2012; Jones and Harrison, 2004; Shaffer and Lighthart, 1997). When looking at atmospheric particles with an aerodynamic diameter of less than 2.5 or 10 µm (which are the fractions routinely measured and studied for health risk assessment, PM2.5 and PM10), it is possible to find viruses, bacteria (agglomerated or not), and spores. However, spores, when produced by fungi, represent the major fraction of PM10 in terms of mass (Elbert et al., 2007). They contribute to the organic aerosol burden of the atmosphere and therefore can affect air quality, as well and weather and climate by influencing cloud and precipitation formation. They can act as ice-nucleating particles (INPs) and can form cloud condensation nuclei (CCN) upon fragmentation in the atmosphere (China et al., 2016; Steiner et al., 2015). Furthermore, bioaerosols can have adverse impacts on human health by acting as pathogens, allergens or toxins (Samake et al., 2017) and play a role in the transmission of crop and animal pests (Fisher et al., 2012).

Bioaerosols include bacteria, fungal spore, pollen and fragments of other organisms, such as plants. The first three groups all include species that can act as CCN or INPs (Fröhlich-Nowoisky et al., 2016), although their activities as cloud nuclei differs per species. The significance of bioaerosol for cloud formation on global and regional scales depends on their abundance, and their relative contribution to INP and CCN populations compared to other aerosol types. On the global scale, their contribution to ice crystal formation is thought to be limited (Hoose et al., 2010; Spracklen and Heald, 2014), although they could still be of importance for cloud formation in specific regions, such as the Amazon.

Estimates of the emissions of bioaerosols on the global scale vary over almost 2 orders of magnitude, which prohibits accurate assessment of their impact on cloud formation and air quality. An early estimate that was based on extrapolation of measurements at a few locations was as high as 1000 Tg yr^{-1} (Jaenicke, 2005). Subsequently, global model simulations have been performed that included parameterizations for three main classes of bioaerosols (i.e., pollen, fungal spores and bacteria). These yielded total emission estimates between 62 and 123 Tg yr^{-1} (Hoose et al., 2010; Myriokefalitakis et al., 2017), with variations between models due to differences in meteorology and land use maps. The variation of estimates for the global bioaerosol burden is large as well, ranging between 121 and 791 Gg and resulting from differences between models in emissions, assumed size distributions and formulation of removal mechanisms. However, the emission parameterizations that are incorporated in these models are based on limited observations. All of the above studies used the same emission schemes, or modified versions thereof. The fungal spore emission scheme of Heald and Spracklen (2009), referred to as HS09 hereafter, is based on measured concentrations of mannitol, a sugar alcohol that is a proxy for fungal spore concentrations, at a limited number of locations, and simulated emissions of fine and coarse spores from all ecosystems as a function of LAI and specific humidity. Myriokefalitakis et al. (2017) used a modified form of the HS09 scheme, based on Hummel et al. (2015). More recently, pollen emission schemes have been developed based on pollen count observations and implemented in regional-scale models (Wozniak and Steiner, 2017; Zink et al., 2013). Finally, the bacteria emission scheme by Burrows et al. (2009) was developed by inverse modeling of measured bacteria concentrations over various ecosystems and assumes constant emissions for each land use

type. Since estimates of the global bioaerosol burden strongly depend on their emissions, emission models that are better constrained by observations are urgently needed.

In this deliverable, we focus on fungal spores, as they have a smaller size than pollen, which implies that they are more likely to be transported over longer distances, and to contribute significantly to the organic aerosol budget on the regional and global scale. Previous studies estimated that fungal spores can contribute around 5 % and 10 % of the mass of PM10 and organic carbon in urban and suburban areas (Bauer et al., 2002, 2008b). In specific environments such as tropical forests, the contribution of fungal spores can represent 45 % of the PM_{10} mass (Elbert et al., 2007). In a study of four Nordic rural sites during the summer, fungal spores were found to be the second most important source of particulate carbon in PM10, contributing 20 %–32% (Yttri et al. 2011), reflecting increased biological activity in the growing season (Yttri et al. 2021). Fungal spores can also produce large quantities of submicrometer fragments after rupturing in the atmosphere and thereby contribute to CCN and INP populations. Many fungal spores contain allergens which can trigger a range of respiratory symptoms in those susceptible. These symptoms include sneezing, runny nose, mucous production, cough, congestion, sinusitis, earache, headache, wheezing, asthma and a range of bronchial symptoms and diseases. It is estimated that around 3-4% of the general population get allergy symptoms from fungal spores, including the majority of asthma sufferers. Many fungal spore types have similar allergens which are released at different times of the year. This means that sufferers of fungal spore allergies are likely to be sensitive to many types for large parts of the year.

Fungi come in a wide range of types and sizes, most are microscopic but some, such as mushrooms and bracket fungi, are quite large. Fungal spores themselves are all microscopic, some as small as two micrometres in size. Most fungi require warmth and humidity to grow, reproduce and release their spores into the environment. Many fungi produce only small amounts of spores which rarely get airborne in quantity. However, some species are very prolific and widespread, producing high concentrations of spores which are readily dispersed into the atmosphere. The main types that trigger most symptoms in allergy sufferers are: Alternaria, Cladosporium, Epicoccum, Aspergillus, Penicillium, Didymella, Pleospora and a group of species collectively referred to as Basidiospores. Also important to asthma sufferers are Sporobolomyces and Tilletiopsis, which are very small spores produced primarily during warm, humid nights. Some example of the typical abundance of different fungal spores species are shown in Figure 1, as averaged over 5 years of observations at the University of Worcester. The concentrations of spores produced by fungi vary greatly from species to species. For example, the Alternaria peak monthly average spore concentration is 3400, while for Cladosporium it is 210,000 and for Didymella 35,000. As a result, the thresholds for symptoms will also vary. However, thresholds have only been ascertained for Alternaria and Cladosporium so far.

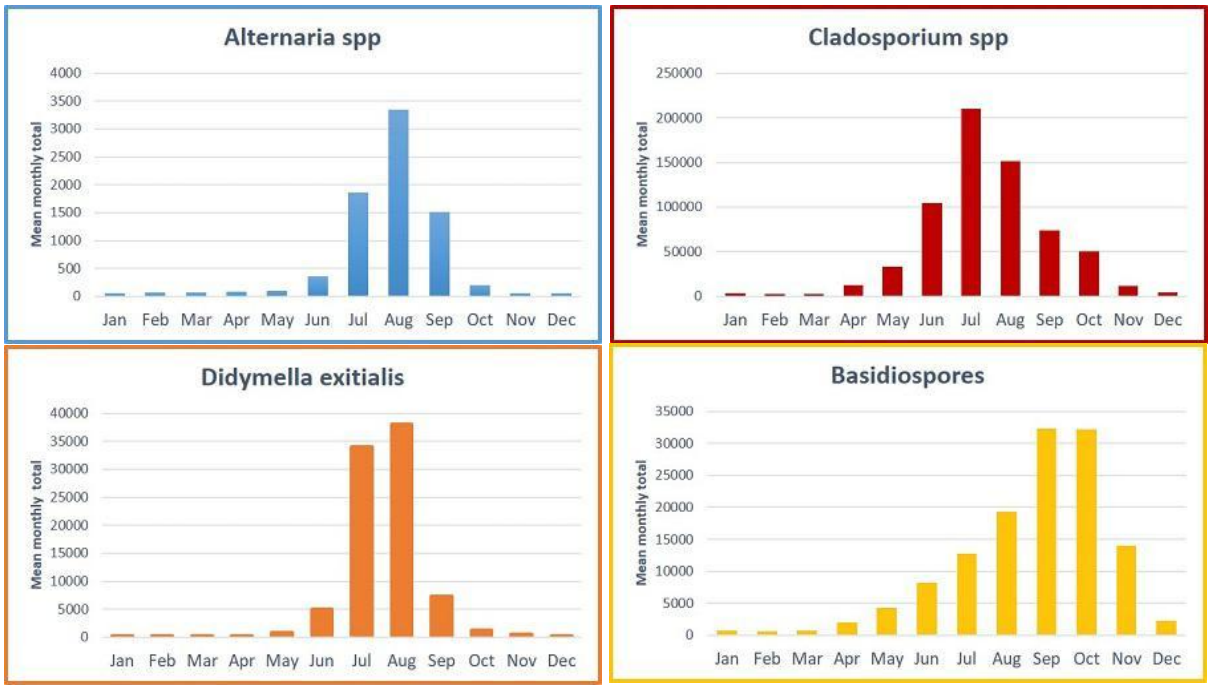

Figure 1. Monthly average totals of spores per cubic metre of air, for the five year period, 2006-2010, as observed by the University of Worcester (UK).

Fungi emit spores into the air as part of their reproductive strategy. These emissions are thought to depend on temperature and water availability (Boddy et al., 2014; Gange et al., 2007; Jones and Harrison, 2004; Löbs et al., 2020), along with biotic factors. Emissions of spores into the atmosphere can be either active or passive, depending on the species of fungus. Active emission mechanisms include emissions at high relative humidity with liquid jets or droplets (Elbert et al., 2007; Pringle et al., 2005). Factors that have been proposed to drive the passive emission of fungal spores into the atmosphere include wind (Jones and Harrison, 2004) and rainfall (Huffman et al., 2013; Prenni et al., 2013). Since the sources of fungal spores are diverse, it is challenging to develop a mechanistic description of their atmospheric emissions, and therefore emissions are usually based on extrapolation of the limited number of available observations. These estimated emissions of fungal spores range widely for different methods, including both models and educated guesses, from 50 Tg yr^{-1} (Elbert et al., 2007), 28 Tg yr^{-1} (HS09), 186 Tg yr^{-1} (Jacobson and Streets, 2009) to 79 Tg yr^{-1} (Sesartic and Dallafior, 2011). Moreover, the seasonal cycle in these estimates is either absent or assumed to be instantaneously related to the seasonal cycle of the driving variables.

4 Implementation of a fungal spores lumped approach in EMEP and IFS-COMPO

This task has mostly focused on implementing and analyzing fungal spores. As summarized in Chapter 7 of the 2024 EMEP report [1], fungal spores make a significant contribution to PBAPs and can also make a significant contribution to PM10. Various fungal spore parameterizations from literature have been implemented in both the regional EMEP model and the global IFS-COMPO model. The model outputs have been compared both to observational data and to each other, as well as to the CHIMERE model. The result of these comparisons are outlined in this chapter.

4.1 Available observations

Direct observations of fungal spores are laborious and time-consuming, and not much data is available. Fortunately, fungal spores are well known to be correlated with certain sugar alcohols, specifically mannitol and arabitol. Mannitol and Arabitol have been measured at various stations in Europe, with some observations in France dating back to 2007. This study uses data from 49 stations across 7 countries, covering the years 2011–2022. These stations include 35 in France, 5 in Switzerland, 3 in Estonia, 2 in Norway, 2 in Italy, 1 in Poland, and 1 in Slovenia. While most stations only have measurements for a year or less, multiple stations in France and Norway have multi-year data. The observations of surface concentration of mannitol and arabitol have been collected by the Institut des Géosciences et de l'Environnement (IGE, Grenoble, France), who kindly made the observations available in the context of the CAMAERA project. The two Norwegian stations are available through the EMEP/EBAS database.

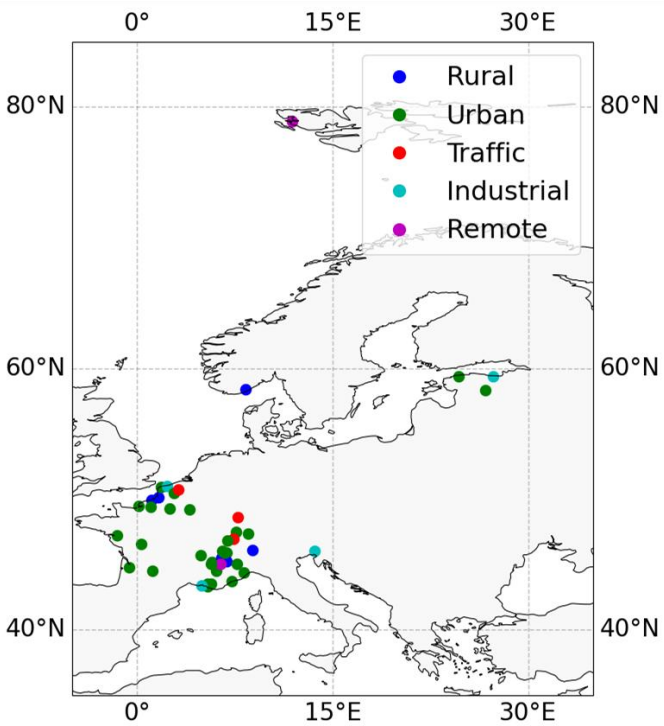

Figure 2. Station with arabitol and mannitol observations, with their classification.

To compare the fungal spore concentration to mannitol and arabitol concentrations, we follow Bauer et al. (2008a), who estimated the average combined mannitol and arabitol content of fungal spores in Vienna to be 2.9 pg per spore. This gives a ratio of arabitol and mannitol mass to spore mass of 20% for lighter spores and 4.5% for heavier spores. We found that the 20% ratio overestimates arabitol and mannitol across all measurements. Therefore, we apply a conversion factor of 4.5% for all parameterizations, consistent with Vida et al. (2024). Assuming a fixed mass ratio of arabitol and mannitol to spore mass (here assumed to be 4.5%), allows to compare simulated spores concentrations with the sugar alcohol observations. Over Europe, most of the observations of arabitol and mannitol are available over France and Norway, kindly provided by IGE Grenoble and NILU respectively. As such, the comparisons mostly focus on the spore concentrations over these two countries.

Janssen et al (2021) use a multi-annual time series (6 years, from 2003 to 2008) of spore counts at 66 stations across the continental USA operated by the American Academy of Allergy, Asthma, and Immunology (AAAAI). Members of the National Allergy Bureau monitor spore and pollen counts at these stations, where samples are collected on at least 3 days a week using a Burkard spore trap. Figure 3 from Janssen et al (2021) show the location of the stations as well as the mean recorded fungal spores concentration over the 2003-2008 period.

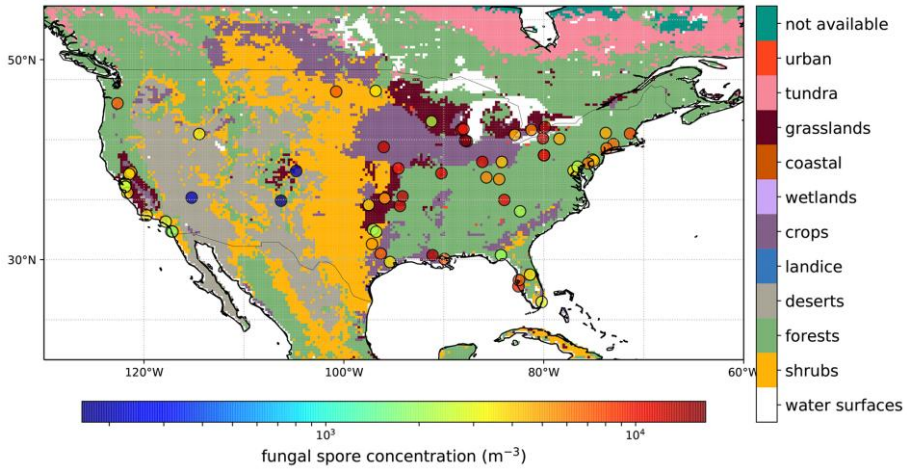

Figure 3. From Janssen et al (2021) Average observed fungal spore concentrations over the period 2003–2008 for all AAAAI stations (circles) shown on top of lumped land use classes bases on the Olson World Ecosystems (Olson et al., 2001).

This dataset is unfortunately not available to use; however, Janssen Ruud from TNO kindly made available a dataset of fungal spores emissions derived from the AAAAI observations of spores concentration, on days without rainfall (as rain can provoke fungal spores emissions as well as removal through wet deposition). That means that we can use a dataset of 3-daily fungal spores emissions over 66 locations in the US, for the years 2003 to 2008.

4.2 Simulating fungal spores in EMEP and IFS-COMPO

Due to the variety of fungal spores species (Elbert et al. 2007, Song et al. 2022), and the relative scarcity of available studies, we do not attempt a speciated analysis of microscopic emission mechanisms for the fungal spores. Instead, we introduce an effective emission flux of spores, using a single monodisperse spore that represents an average airborne spore. Various parameterizations for such effective spore fluxes exists in the literature, as reviewed by Myriokefalitakis et al. (2017) and Vida et al. (2024). In its simplest form, the fungal spore

flux depends solely on the ecosystem type, as parameterized by Sesartic and Dallafior (2011), based only on land-use classes. However, correctly incorporating seasonal variability requires a more sophisticated approach. Using mannitol concentrations in combination with the GEOS-Chem model, Heald and Spracklen (2009) found that fungal spores are strongly correlated with both the Leaf Area Index (LAI) and specific humidity at the surface (q) and derived a fungal spores emission scheme which applies to particles of 5 micron. Building on these results, Hummel et al. (2015) modified this parameterization to apply to spores with a diameter of 3 µm. Additionally, Hummel et al. (2015) proposed an alternative fungal flux parameterization for 3 µm spores that also accounts for surface temperature, T [◦C], by fitting observations of fungal spores concentration over 3 sites in Europe. Finally, Janssen et al (2021) derived a fit between the fungal spores emission fluxes derived from AAAAI observed fungal spores counts and LAI, q, surface temperature (T) and friction velocity (u*). These three parameterizations of fungal spores emission fluxes (F_{Js} for Janssen et al 2021, $F_{H\&S}$ for Heald and Spracklen 2009 and F_{Hm} for Hummel et al 2015) are shown in Figure 4:

$$F_{\mathrm{Js}} = 2.63 \times 10^{-5} + 6.1 \times 10^{3} \times \overbrace{q}^{\text{Specific humidity [kg/kg]}} + 46.7 \times \overbrace{\mathrm{LAI}}^{\text{Leaf-area index [m}^2\text{/m}^2\text{]}} + 59.0 \times \underbrace{u^*}_{\text{Friction velocity [m/s]}} \quad [\text{Ref. 1}]$$

$$F_{\mathrm{H\&S}} = c \times \frac{\overbrace{q}^{\text{Specific humidity [kg/kg]}}}{7.5 \cdot 10^{-2}} \times \overbrace{\mathrm{LAI}}^{\text{Leaf-area index [m}^2\text{/m}^2\text{]}}, \quad c = \begin{cases} 2315\ \mathrm{m^{-2}\ s^{-1}} & d = 3\ \mu\mathrm{m} \quad [\text{Ref. 2}] \\ 500\ \mathrm{m^{-2}\ s^{-1}} & d = 5\ \mu\mathrm{m} \quad [\text{Ref. 3}] \end{cases}$$

$$F_{\mathrm{Hm}} = 20.426 \times (\overbrace{T}^{\text{Temperature [}^\circ\text{C]}} - 275.82) + 3.93 \times 10^{4} \times \overbrace{q}^{\text{Specific humidity [kg/kg]}} \times \underbrace{\mathrm{LAI}}_{\text{Leaf-area index [m}^2\text{/m}^2\text{]}} \quad [\text{Ref. 4}]$$

Figure 4. Specifics of the three fungal spores emission schemes implemented and tested in EMEP and IFS-COMPO. The Janssen et al (2021) parameterization has not been tested in the EMEP model.

4.2.1 Subsequent adjustments of the fungal spores emission fluxes in EMEP

Within the EMEP model, the best agreement was found for the parameterization from Heald and Spracklen (2009). This parameterization depends linearly on both the humidity and leaf-area index. The parameterization assumes a spore diameter of 5µm, and is therefore referred to as HS-5 in what follows.

As shown below and in the 2024 EMEP report, within EMEP this parameterization produces excellent results for France but severely overestimates the spore concentrations in Norway.

Several attempts have been made to modify the parameterization from Heald and Spracklen in EMEP, to better reflect Norwegian observations, including:

- Cutting off emissions below a fixed temperature.
- Cutting off emissions once there is snow cover.
- Reducing the emissions from coniferous trees.

Whilst these measures improve the agreement with the Norwegian observations, they also generally worsen the agreement with the French observations. As a consequence, the parameterization from Heald and Spracklen (2009) continues to be used in the subsequent comparison. The work to improve the parameterization in EMEP to more accurately reflect the Norwegian observations is however ongoing.

A more complete evaluation of the EMEP simulated fungal spores is presented in Sectin 5.

4.2.2 Subsequent adjustments of the fungal spores emission fluxes in IFS-COMPO

Similarly to what has been tested in the EMEP model, no fungal spores emissions occur when snow is present, for all emission schemes. A temperature threshold of 5°c for the occurrence of fungal spores emissions has been implemented. Janssen et al (2021) showed in their supplement the strong and positive impact of a temperature threshold on fungal spores emissions (see Figure 5).

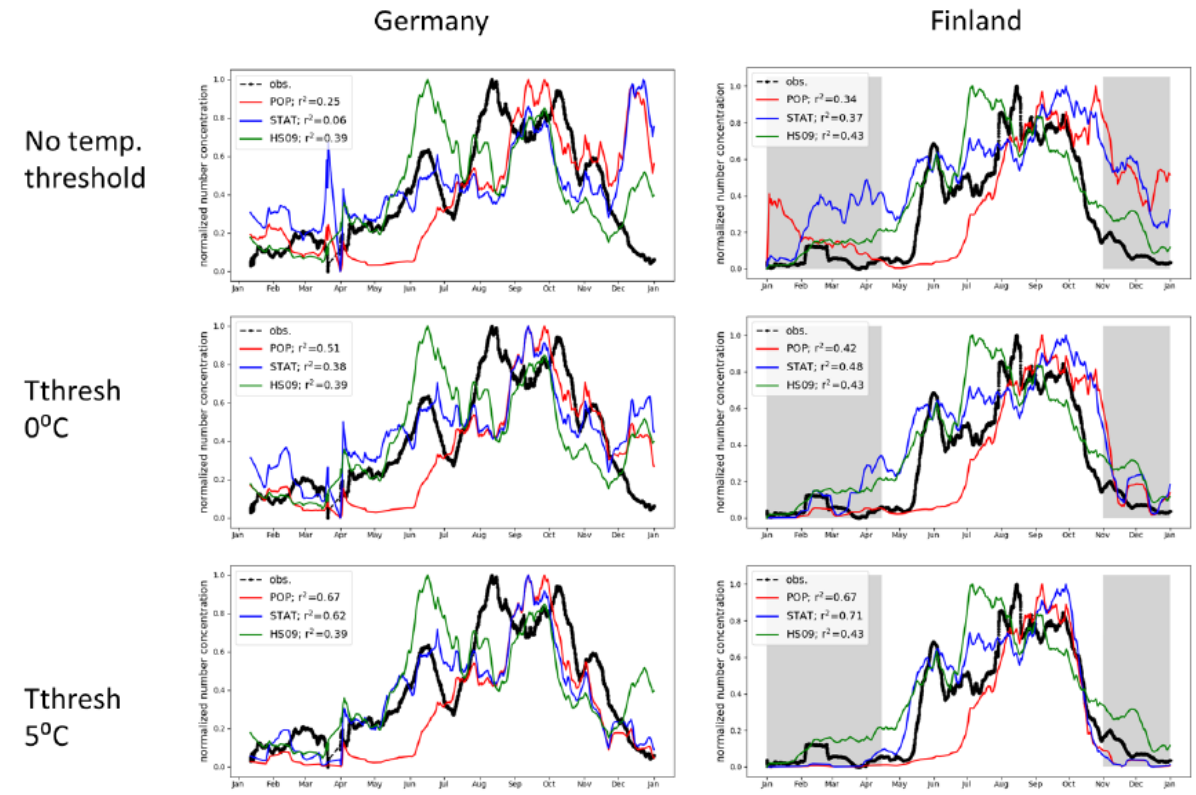

Figure S5: sensitivity to chosen temperature threshold of modeled spore concentrations at the sites in Germany and Finland. No temperature threshold (top), threshold of 0°C (middle) and threshold of 5°C (bottom)

Figure 5. From the supplement of Janssen et al (2021) : simulated and observed fungal spores concentration over stations in Germany and Finland, as simulated by the Heald and Spracklen emission scheme (green), the Janssen et al 2021 statistical model (blue) and the Janssen et al 2021 population model (red), using no temperature threshold for fungal spores emissions (top), a 0° temperature threshold (middle) and a five degree emissions threshold (bottom).

Also, following an evaluation of the simulated fungal spores concentration against surface concentration of arabitol and mannitol and of the fungal spores emission fluxes against the derived emissions from Janssen et al (2021), a scaling has been applied to the Hummel et al (2015) and Janssen et al (2021) emission schemes in order to reduce systematic biases between the IFS-COMPO simulated values and the observations. This scaling improved

significantly the simulated values, as shown in Figure 6 for the IGE station at Grenoble (France).

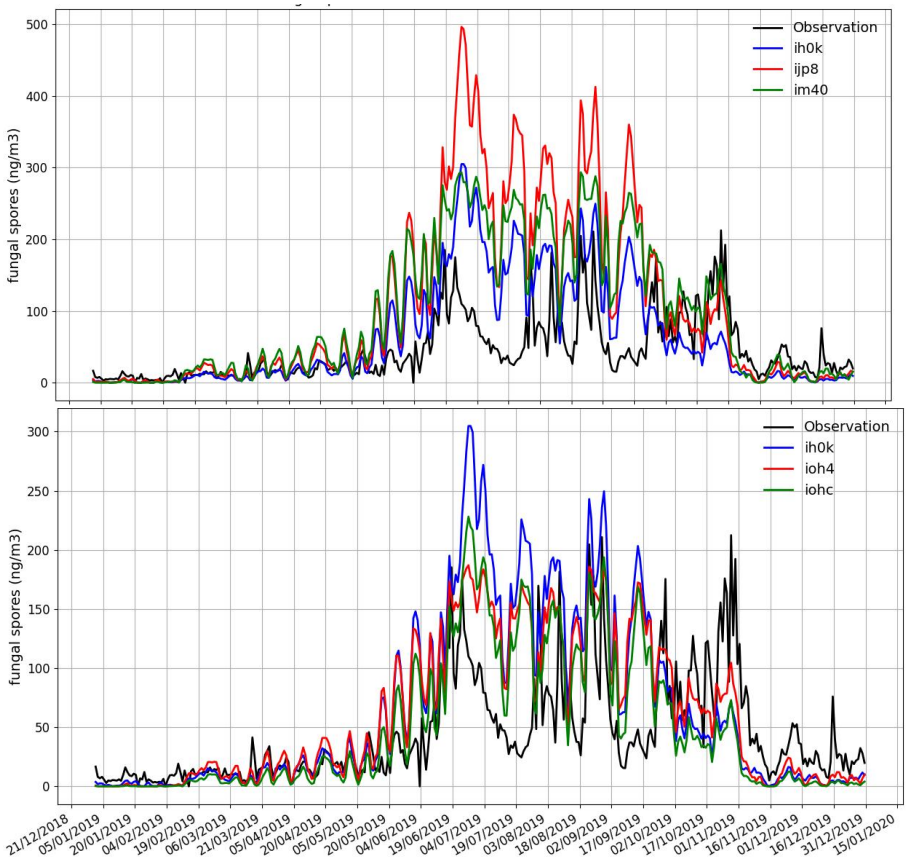

Figure 6. Observed (black) and simulated (blue=HS09, green=J21/J21 adjusted, red=H15/H15 adjusted) surface concentration of fungal spores in 2019 at Grenoble (France). First set of simulations (top); adjusted simulations (bottom).

A more complete evaluation of the IFS-COMPO simulated fungal spores is presented in Section 6.

4.2.3 Treatment of fungal spores optics in IFS-COMPO

In EMEP, fungal spores are transparent : they don't interact with light and radiation through scattering or absorption, this is not the case in IFS-COMPO. A set of refractive indexes have been found for fungal spores from laboratory measurements (Ding et al 2023), and the ecaeropt Mie code of ECMWF has been run using these refractive indexes to compute the fungal spores mass extinction, single scattering albedo (SSA) and asymmetry parameter, assuming that fungal spores are homogeneous spheres with a 3 micron modal diameter, 1.2 geometric standard deviation and 1000 kg/m^3 density. Fungal spores are also supposed to be hydrophobic. The results are shown in Figure 7, together with the refractive index used. As compared to other species, the mass extinction of fungal spores in very low, which is consistent with the size assumption and the assumed real part of the refractive index which is lower than for most of other IFS-COMPO aerosol species. On the other hand, the SSA is very low, comprised between 0 and 0.5 depending on the wavelength. This means that although fungal spores are unlikely to contribute much to simulated aerosol optical depth (AOD), they could contribute significantly to the simulated SSA and absorption aerosol optical depth (AAOD).

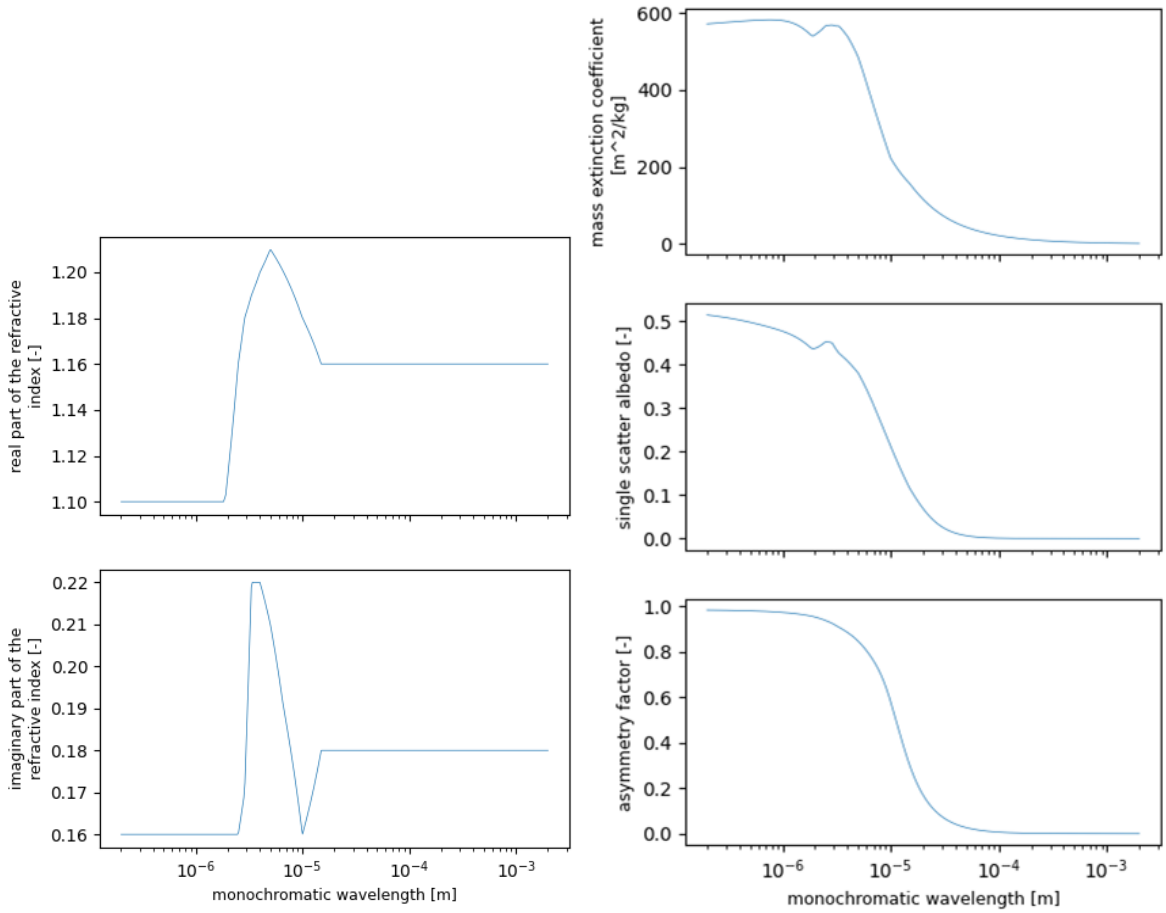

Figure 7. Fungal spores optics implemented in IFS-COMPO as a function of wavelength. Left, real (top) and imaginary (bottom) part of the refractive index. Right, from top to bottom, mass extinction, single scattering albedo and asymmetry parameter.

5 Results with EMEP

This section has also been reported in the 2024 EMEP report.

5.1 Comparison of different emission schemes for the year 2017

The different parameterizations were compared for the year 2017, as it has the most available observations. The monthly means, averaged over all stations, are shown in Figure 8 (a). In Figure 8 (b), we also show how total PM10 is modified by the different parameterizations. The monthly average normalized mean bias (NMB) for the various stations and parameterizations are shown in Figure 9.

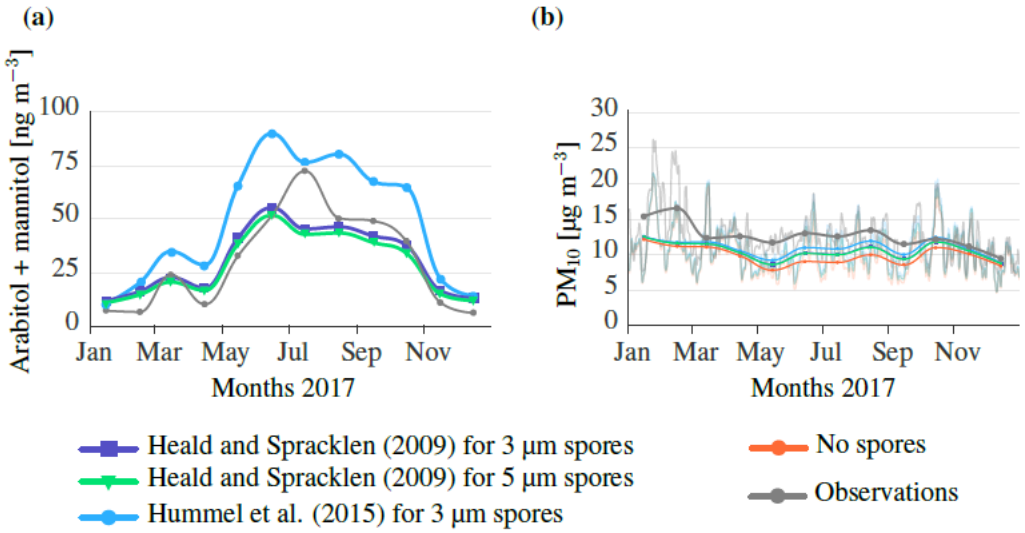

Figure 8. Comparison of spore parameterizations for monthly averaged values in 2017, showing (a) combined arabitol+mannitol and (b) total PM10.

All three parameterizations tend to overestimate the spore contribution in Norway, as discussed further below. The Hummel et al (2015) parameterization shows a high correlation with the measurements but severely overestimates spore concentrations. Overall, the parameterization from Heald and Spracklen (2009) performs the best. The 3 µm and 5 µm spore parameterizations show comparable results, but the 5 µm parameterization has a slightly smaller bias, and the spore mass aligns more closely with the mannitol and arabitol ratios reported by Bauer et al. (2008a). Therefore, this parameterization is used for all subsequent runs discussed in this chapter. The impact on simulated PM10 is positive in the sense that a systematic low bias of simulated values is reduced from April to October.

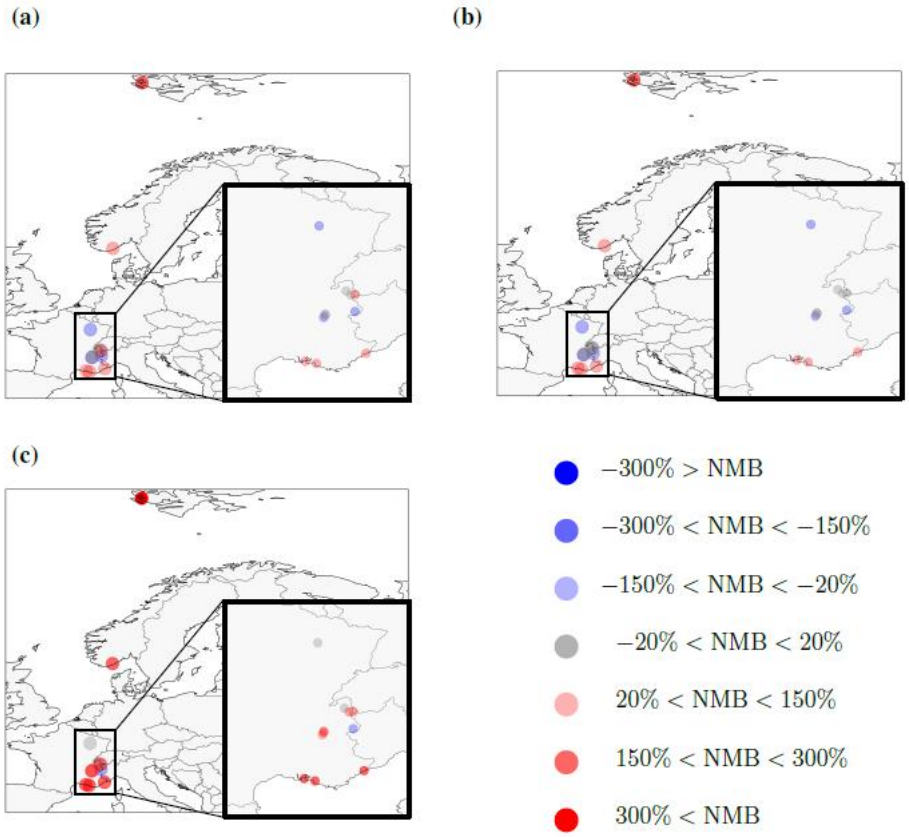

Figure 9. Monthly averaged normalized mean bias (NMB) for the year 2017, using various fungal spores emissions parameterizations. (a) The parameterization from Heald and Spracklen (2009) for spores with a diameter of 3. The overall NMB is 10.1 %. (b) The parameterization from Heald and Spracklen (2009) for particles with a diameter of 5 µm. The overall NMB is 1.5% (c) The parameterization from Hummel et al. (2015) for spores with a diameter of 3 µm. The overall NMB is 71.8 %.

5.2 2011-2022 simulations with the EMEP model

We ran the EMEP model on a coarse 0.3 ◦ ×0.2 ◦ grid for the years 2011 to 2022, corresponding to the available observations. We show results for monthly averages in Figure 10, and selected weekly averages in Figure 11. In this section, weekly averages are included only if the observations cover at least two days of the week, and monthly averages are included only if the observations span at least five days across two different weeks of the month.

5.2.1 Monthly evaluation

The total monthly averages for all stations are shown in Figure 10 (a) for both the observations and model outputs. A clear seasonal variation is observed, with significantly higher spore concentrations during the summer. The country-resolved bias is illustrated in Figure 10(b), showing that the model significantly overestimates spore concentrations in Norway but has a low bias in France. Finally Figure 10(c)–(d) shows the data for ANDRE-OPE and Birkenes Observatory, respectively, which are the French and Norwegian stations with the most available observations.

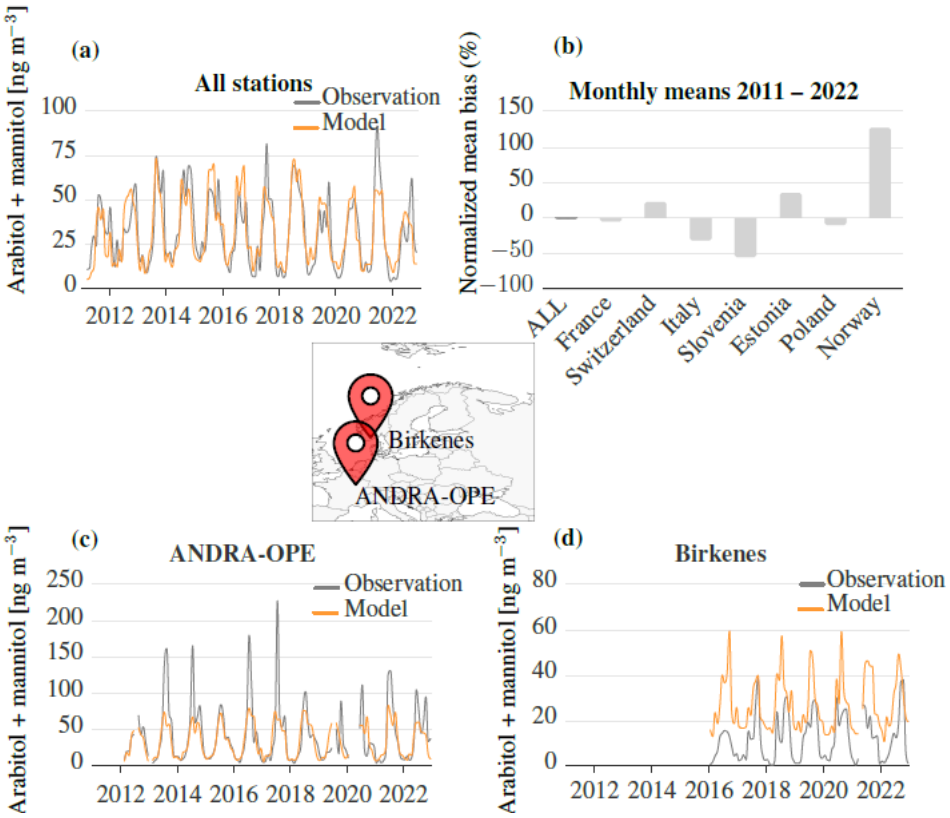

Figure 10. Comparison of the monthly mean of the EMEP model output with monthly mean observational data, using the parameterization from Heald and Spracklen (2009) for 5 µm spores containing 4.5% arabitol + mannitol, with (a) monthly means of all observations and (b) country-resolved normalized mean bias. Note that countries other than Norway and France only include few observations. In (c), we show the French station with most observations, where the model slightly underestimates the spore concentration, whereas (d) shows the Norwegian station with most observations, where the model significantly overestimates the spore concentration.

5.2.2 Weekly evaluation

To gain insight into finer-scale variations, we also show the weekly averages for a single year in Figure 11, for the same stations as in Figure 9. The general pattern of higher fungal spore concentrations in summer is well captured, but some features are missing, such as the peak and subsequent dip in June at the Birkenes Observatory.

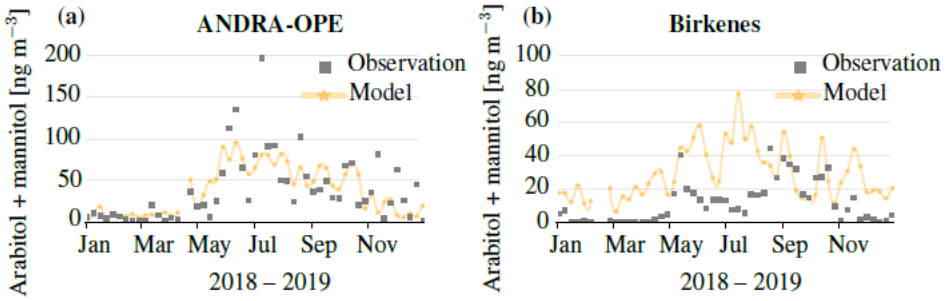

Figure 11. Comparison of weekly means between the EMEP model and observations for the two stations shown in Figure 9.

5.2.3 Statistical evaluation

Finally, we show the normalized mean bias, as well as the spatial and temporal correlations across all observations for both monthly and weekly data in Table 1. The results show a slightly lower bias for the monthly data, but the correlations are comparable between the two time scales. We also include a comparison to PM10 for the year 2022, similar to the analysis shown for 2017 in Figure 9. As the EMEP model consistently underestimates PM10, the improvement in NMB is expected. Encouragingly, the correlations remain high and even show slight improvement.

Table 1: Statistics to evaluate the fungal spore parameterization from Heald and Spracklen (2009) for 5 µm spores, showing the number of included observations, Nobs, the normalized mean bias (NMB), the spatial (R-space) correlation, and the temporal (R-temporal) correlation. For the PM10 monthly statistics, only stations with at least 21 days in three different weeks are included. The data is collocated and statistics are computed using pyaerocom and AeroVal (AeroTools 2024).

	N_{obs}	NMB (%)	R-space	R-temporal
Weekly arabitol + mannitol (2011–2022)	940	−2.8	0.73	0.76
Monthly arabitol + mannitol (2011–2022)	1047	−0.8	0.72	0.77
Monthly PM_{10} without spores (2022)	735	−8.0	0.78	0.64
Monthly PM_{10} with spores (2022)	735	−2.8	0.79	0.67

The overall performance of the model in simulating spore concentrations is encouraging, with a generally low bias and high correlation with observed data. The model successfully captures the broad seasonal trends, although significant regional differences suggest areas where improvements are needed. In Norway, the model significantly overestimates spore concentrations, especially during winter (see Figure 10(d)). This overestimation is likely related to the model's reliance on the Leaf Area Index (LAI) for parameterization. In the region around the Norwegian station, there is a high prevalence of coniferous trees, which maintain a relatively stable LAI throughout the year. As a result, the model predicts non-zero spore concentrations even in winter, despite observations indicating almost no spores. This issue is not observed at French stations, where the surrounding vegetation primarily consists of deciduous forests, crops, and grassland, all of which exhibit much lower LAI in winter. Additionally, different fungal species are likely prevalent across Europe, meaning that the results by Bauer et al. (2008b), based on results in Vienna, may not be representative for all of Europe.

6 Results with IFS-COMPO

6.1 Experiments

A series of specific branches, including the new lumped fungal spores species and various emission schemes, has been developed on top of IFS-COMPO cycle 49R1. Corresponding forecast only experiments (ie without data assimilation) have been run for the years 2017 and 2019, using the usual CAMS resolution of $T_L511L137$ (40 km grid cell). The experiments are called "HS09", "H15" and "J21" respectively for those using the Heald and Spracklen (2009), Hummel et al (2015) and Janssen et al (2021) emission schemes. The H09 scheme has been tested in its 3 and 5 micron variants. Also, the H15 and J21 experiments where the fungal spores emissions have been scaled to be closer to observational data are included in the evaluation and names "H15 adjusted" and "J21 adjusted".

6.2 Global budgets

Table 2 summarizes the global production and deposition terms for the newly introduced fungal spores tracer. For production, HS09 (3 and 5 micron), J21, J21 adjusted and H15 adjusted are all between 40 and 60 Tg per year, while the H15 parameterization gives much higher emissions. Those values are higher than report for HS09 in Janssen et al (2021) : 31 Tg per year production, and for their statistical model, with only 3.7 Tg per year emissions. For the HS09 scheme, the differences can arise from different values of the inputs, notably LAI which is very variable from one dataset to another. Because fungal spores are large particles, sedimentation is the dominant sink for all experiments; wet deposition represents between 30 and 40% of total deposition. The simulated burden is relatively small, between 0.14 and 0.21 Tg except for H15 with 0.57 Tg, and the lifetime varies between 1.2 and 1.6 days, which is in line with other studies : Janssen et al (2021) report 1.4 days lifetime for their statistical model, and 1.1-2.6 days lifetime for HS09. Global emissions and burden follow a seasonal cycle, with a maximum in summertime for all schemes, associated with larger areas with high LAI.

Table 2. Fungal spores global emissions and deposition budgets for the various fungal spores IFS-COMPO experiments. The burden and lifetime are also shown.

Model name	Emissions (Tg/Yr)	Dry deposition + Sedimentation (Tg/Yr)	Wet deposition (Tg/Yr)	Burden (Tg)	Lifetime (days)
HS09 (3 micron)	47.2	29.4	17.8	0.19	1.47
HS09 (5 micron)	63	42.3	20.7	0.21	1.21
H15 (native)	142.3	91.2	51.1	0.57	1.46
H15 (adjusted)	37.2	23.7	13.5	0.16	1.57
J21 (native)	65.7	47.4	18.3	0.22	1.22
J21 (adjusted)	38	25.5	12.5	0.14	1.34

6.3 Simulated surface concentration and PM10 fraction

Figure 12 shows the mean simulated surface concentration of fungal spores by the three HS09 (5 micron), H15 adjusted and J21 adjusted experiments, for a winter and a summer month. In wintertime, surface concentration above 1 µg/m^3 are found mostly over tropical and equatorial evergreen forests in Africa, Amazon and South East Asia. The simulated values range between 4 and 10 µg/m^3 over these areas depending on the emission scheme. In summertime, the simulated values are quite close over these areas, a bit higher with the HS09 scheme (12-15 µg/m^3). The mean simulated values vary between 2 and 5 µg/m^3 over extra tropical forested areas, such as over Europe, Siberia, Eastern US, parts of Canada and China, with higher values with the HS09 experiments.

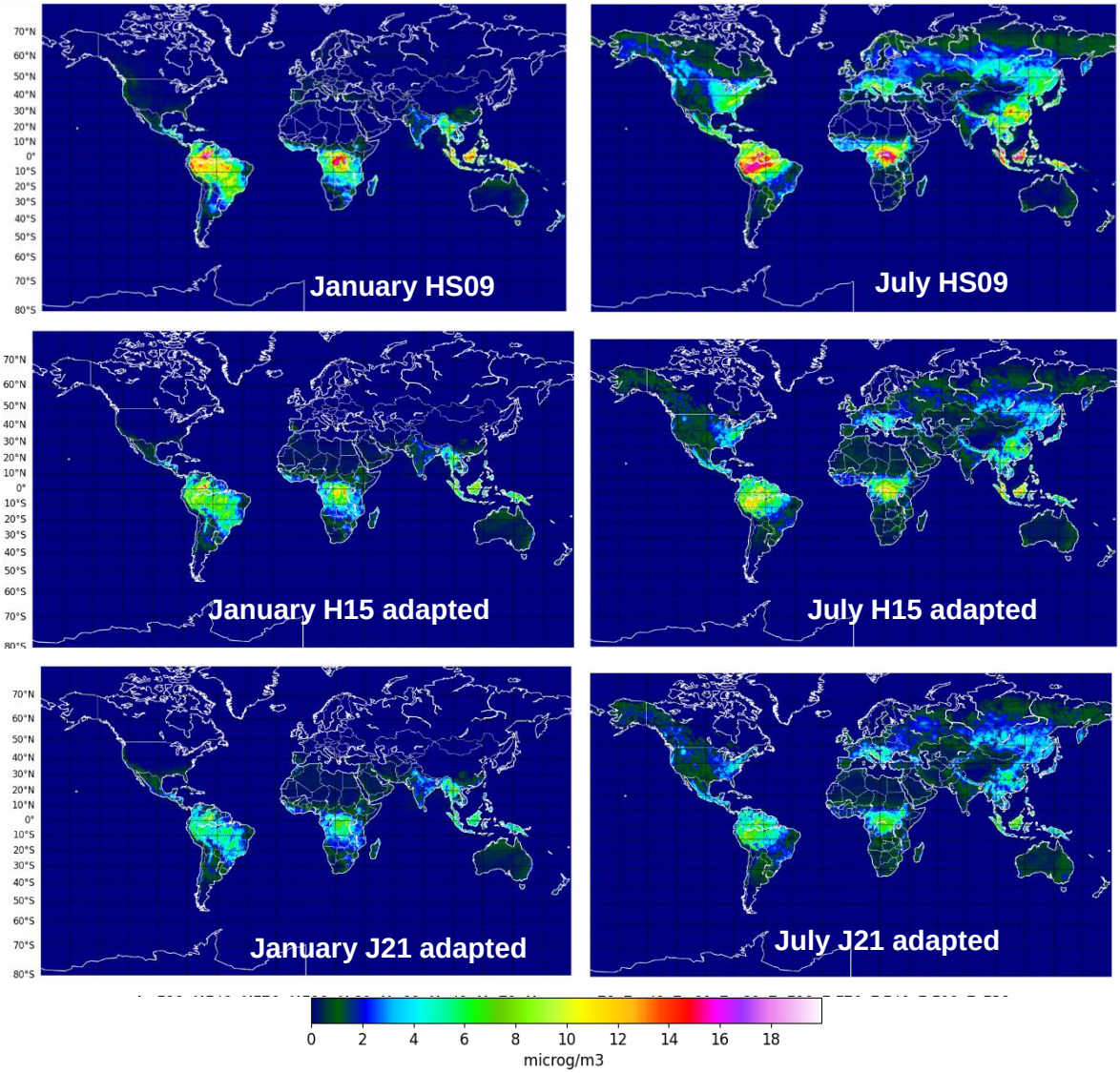

Figure 12. January (left) and July (right) 2019 simulated fungal spores surface concentration, using HS09 (5 micron), top, H15 adjusted (middle) and J21 (bottom).

Figure 13 shows the relative increase in simulated PM10 arising from the effect of including fungal spores, in winter and summer months, and for the three same emissions scheme as in Figure 12. Over tropical and equatorial forests, PM10 is increased by 50 to more than 100% (as over the Amazon with HS09 for example). In wintertime, the contribution of fungal spores

over extra tropical regions PM10 is small, as expected. In summertime, depending on the scheme and the region, the simulated PM10 is increased over extra tropical forested regions by 10 to 40%, with higher values over Eastern US, parts of Canada, central Europe and Siberia.

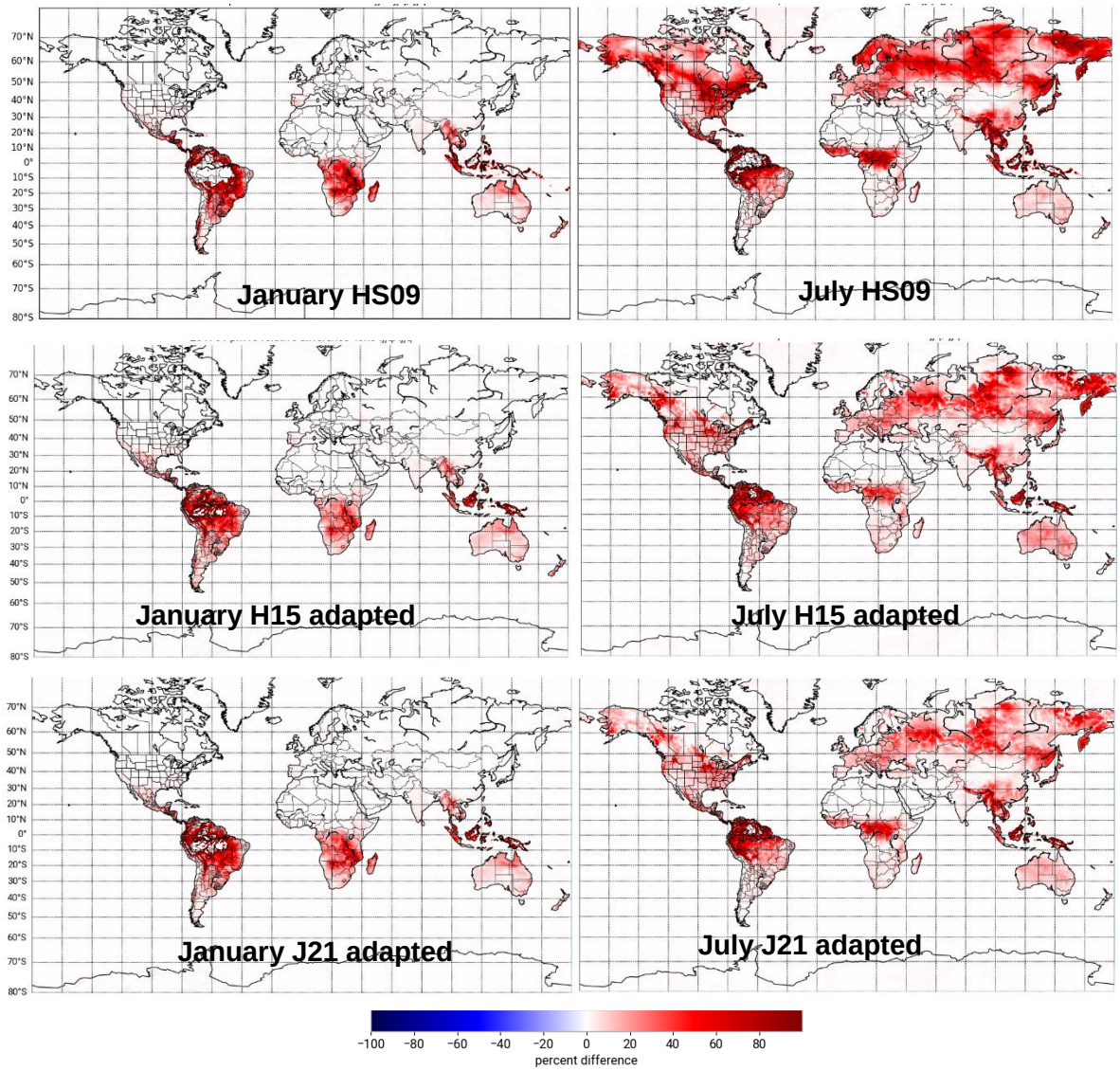

Figure 13. Relative PM10 difference in percentage as compared to simulations without fungal spores. Left, January 2017, right, July 2017. HS09 (5 micron), top, H15 adapted, middle, J21 adapted, bottom. A value of 80% means that PM10 is simulated to be 80% higher.

6.4 Evaluation

In this section, we evaluate the simulated fungal spores related variables (surface concentration, emissions, PM10 and single scattering albedo) against observational datasets.

6.4.1 Arabitol and mannitol surface concentration

The arabitol and mannitol dataset kindly provided by the IGE has been used, using a 4.5% fraction of fungal spores assumed to be arabitol+mannitol, as done for the EMEP evaluation showed in Section 5. The HS09 (5 micron variant) together with the adjusted versions of the H15 and J21 experiments are shown. Figure 14 shows the simulated and observed values in 2019 over two stations in France: Lyon and Grenoble. Both stations show several observed peaks above 100 ng/m^3: in June, August, September and late October/early November. The simulated values reproduce more or less the timing of these peaks, although they often overestimate as compared to observations. HS09 in particular is clearly overestimating, while this is less the case for the adjusted H15 and J21 simulations, particularly over Lyon. The autumn peak is simulated but with a clear underestimation.

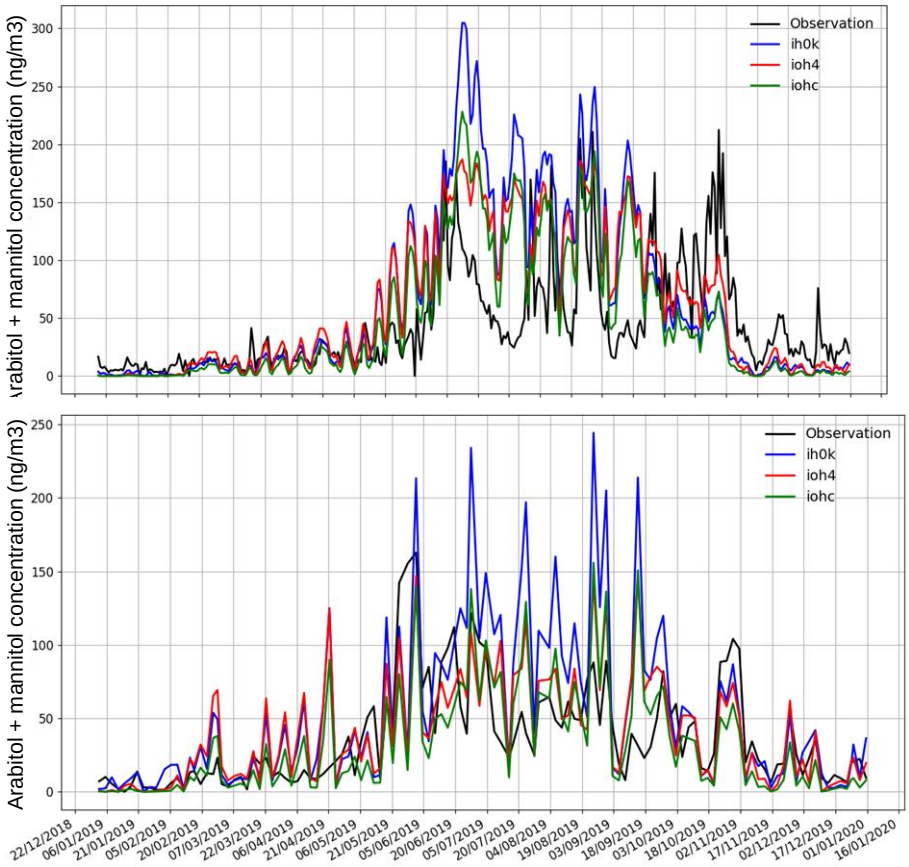

Figure 14. Simulated and observed arabitol+mannitol surface concentration in 2019 over Grenoble (top) and Lyon (bottom) in France. **Blue is HS09**, **green is H15 adjusted**, **red is J21 adjusted**.

Figure 15 shows aggregated skill scores over the the year 2019, for all stations. The three experiments show a similar correlation, between 0.59 and 0.62. The mean bias is positive for HS09, slightly negative for H15 adjusted, and slightly positive for J21 adjusted. However, these mean values hide a wide variety of values, from common underestimation in wintertime and autumn, when the observed values are often low, to frequent overestimation in summertime. The RMSE is higher for HS09 than for the other two experiments.

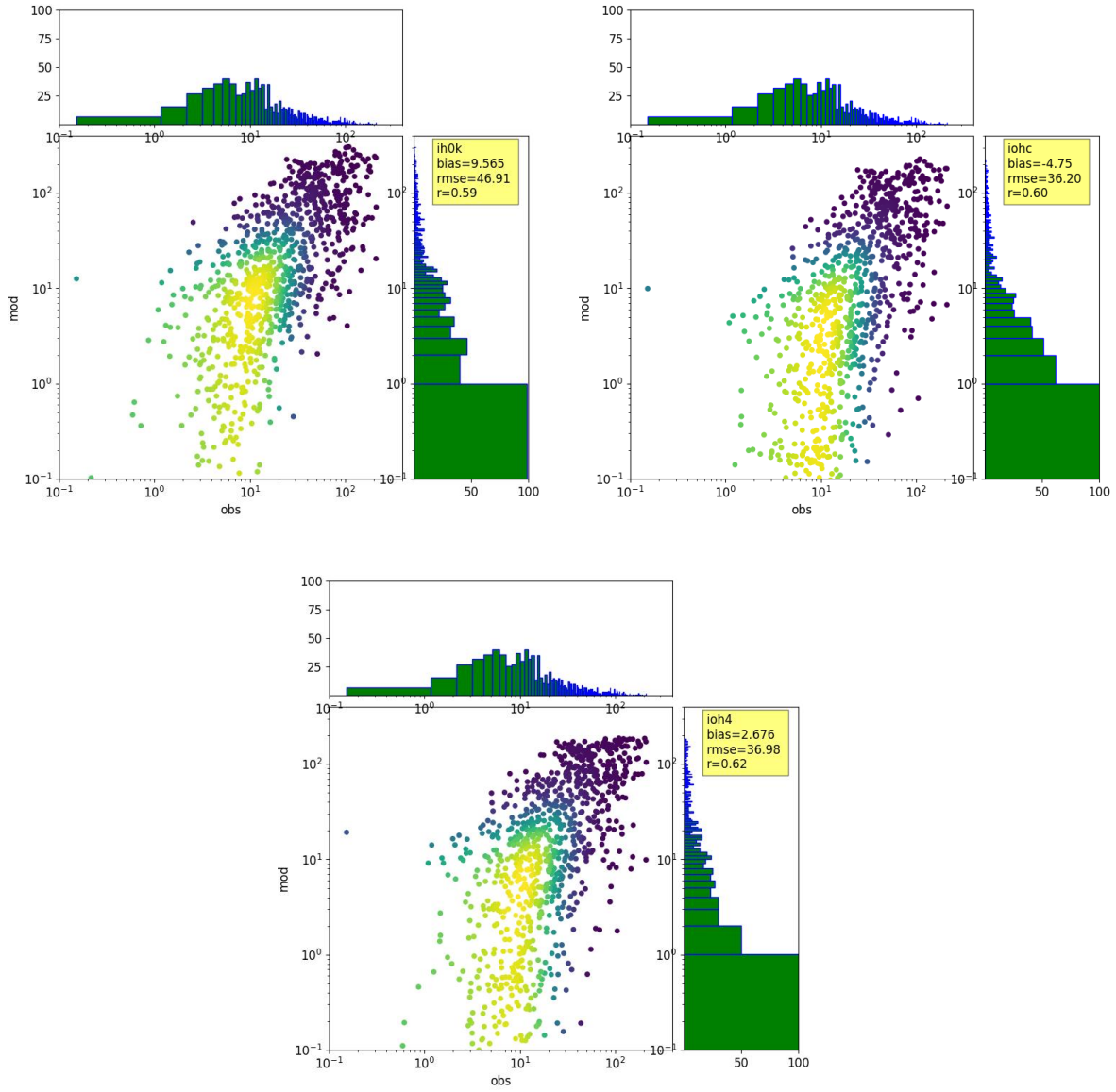

Figure 15. Density scatterplots of all arabitol+mannitol observation/simulation surface concentration in ng/m^3 couples in 2019. HS09 (top left), H15 adjusted (top right) and J21 adjusted (bottom).

6.4.2 Fungal spores emission fluxes

In this section, simulated and retrieved fungal spores emissions over the U.S. are compared. The fungal spores emission fluxes derived from AAAAI observations of fungal spores counts as kindly provided by R. Janssen are originally in counts per m² per second. In order to compare against simulated values which are in units of mass, not in counts, an assumed 2.5 micron diameter of fungal spores is used. The resulting dataset covers the years 2003 to 2008; a comparison between simulated values in July 2019 and derived ones in July 2006 is shown in Figure 16.

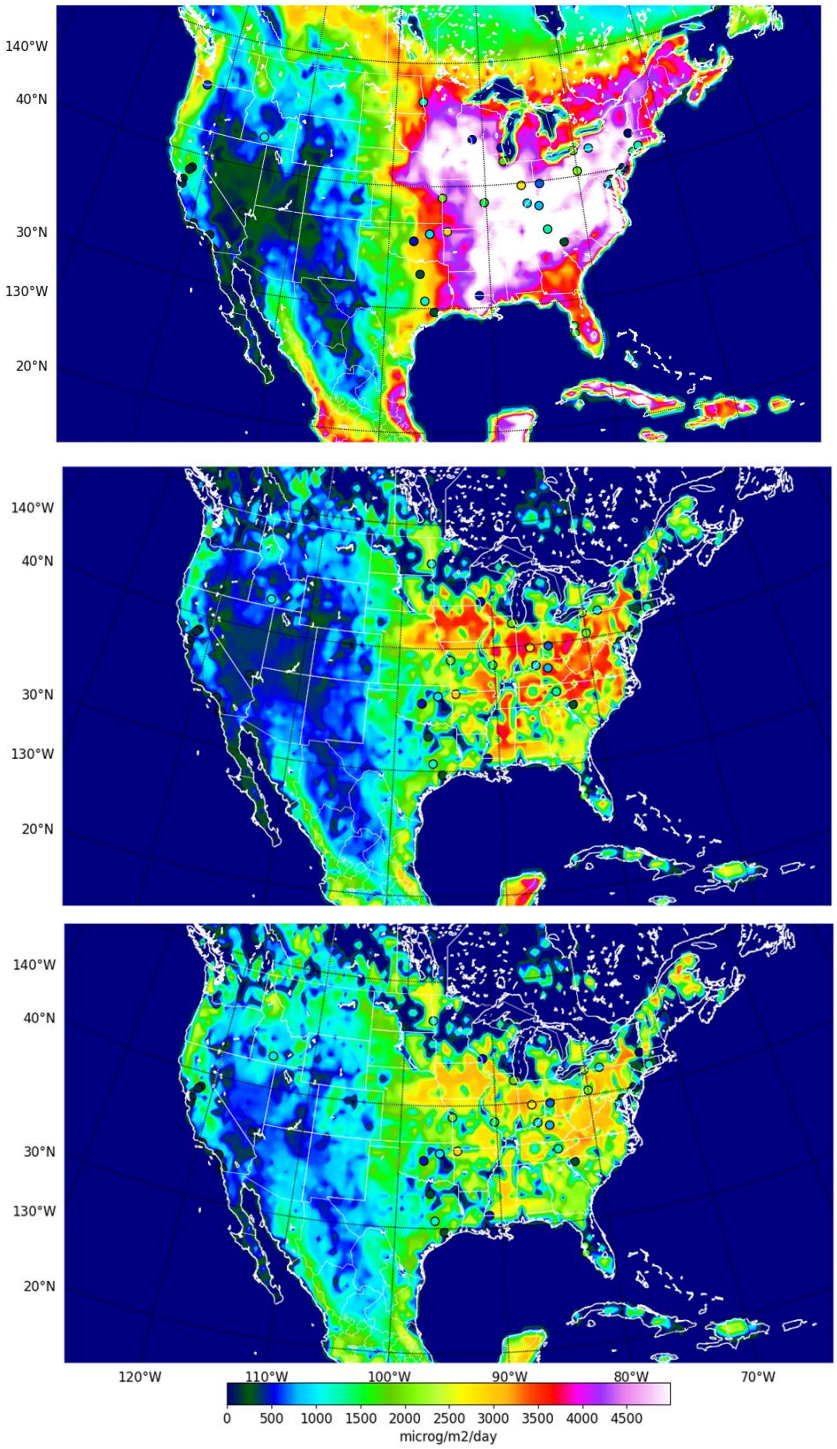

Figure 16. Fungal spores simulated emissions in July 2019 compared to emissions derived from observations in July 2006. HS09 (top), adjusted H15 (middle) and J21 (bottom).

The derived fungal spores emission are of course quite dependent on the assumed size distribution of each fungal spores. However, the 2.5 micron value comes from observations of fungal spores size distribution reported in Perring et al (2015) and in Janssen et al (2021), and are shown in Figure 17.

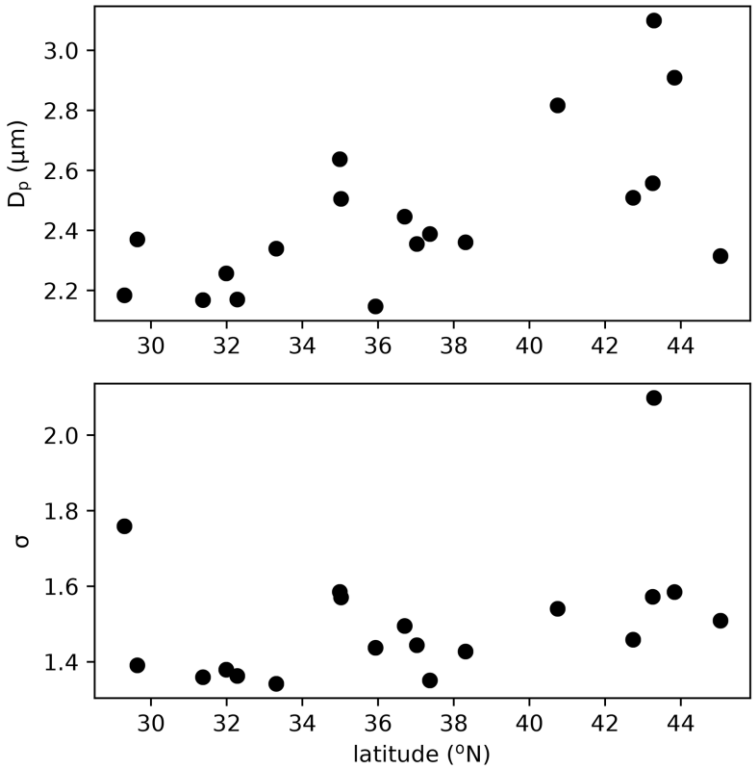

Figure 17. From Janssen et al (2021): Geometric mean diameter (D_p) and geometric standard deviation (σ) as a function of latitude for the number distribution of fungal spores particles observed over the continental USA in 2016.

The estimated fungal spores emissions by the HS09 scheme appear to be very much overestimated, with simulated values 4000 to 5000 µg/m²/day over much of Eastern US against 1000 to 2000 µg/m²/day observed. The adjusted H15 also shows too high values, over 3000 to 4000 µg/m²/day over the same area while the adjusted J21 is quite close to observed values. Figure 18 shows the mean monthly simulated and retrieved fungal spores emission fluxes, averaged over West and East US. Both observed and simulated values are significantly higher over Eastern US than West US, because of the higher forest cover. The observational yearly spread is quite significant, and over Eastern US the observed maximum fungal spores emissions occur in October, while over West US, a plateau of high emissions occur (on average) between June and November. The simulated values struggle to reproduce the observed seasonal cycle; in particular the higher emissions in September-October are underestimated, which is consistent with the results of the evaluation versus European observations of sugar alcohols and, over West US, the summertime emissions are overestimated. The HS09 scheme shows much too high emissions except in wintertime.

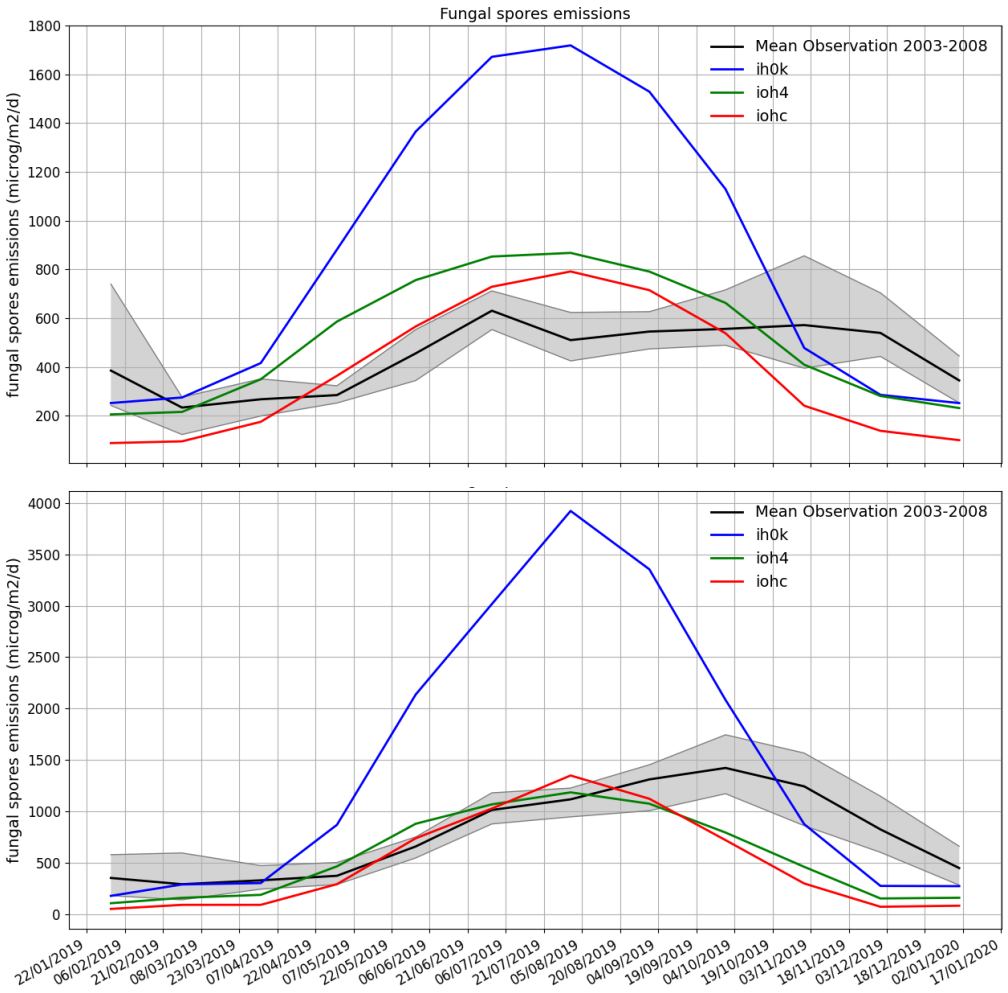

Figure 18. Simulated (in 2019) and observed (from 2003 to 2008 envelope in gray, with mean value in black) over West U.S. (top) and East U.S. (bottom). **Blue is HS09**, **green is J21 adjusted**, **red is H15 adjusted.**

Finally, Figure 19 examines the simulated and retrieved fungal spores emission fluxes over three AAAAI stations in Ohio, Texas and Oklahoma. The yearly variability of the observations is quite different : moderate over Dayton and Tulsa, and very high over College Station. The observed maximum occurs, on average, at different dates in the year: in early Autumn over Dayton and College station (but it occurred also in May for a given year at the latter station), and in June at Tulsa. Interestingly, the simulated timing of the emissions peak differs also from site to site: in July at College station, in August in Dayton and in June at Tulsa. HS09 brings way too high emissions at all three stations, while the other two experiments overestimate in Dayton, underestimate in Tulsa, and show no strong systematic bias (but a shift in the timing of the peak emissions) at College station.

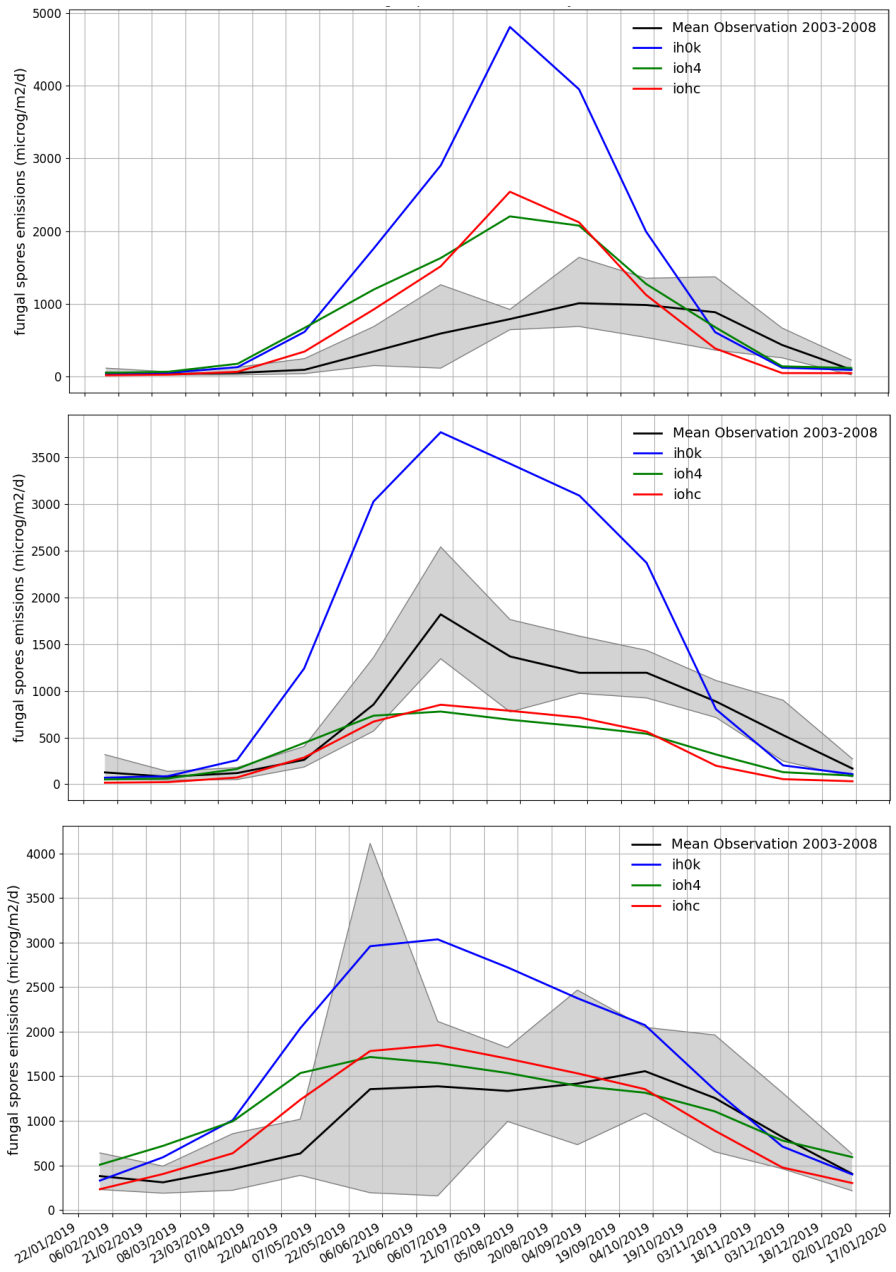

Figure 19. Simulated (in 2019) and observed (from 2003 to 2008 envelope in gray, with mean value in black) over Dayton, Ohio (top), Tulsa, Oklahoma (middle) and College station, Texas (bottom). **Blue is HS09**, **green is J21 adjusted**, **red is H15 adjusted.**

6.4.3 PM10

Evaluating the impact of fungal spores of PM10 is at the same time indispensable, as PM10 is known to be impacted by fungal spores in relevant places and seasons, and tricky because as PM10 includes all species, it can be hard to detect the impact of fungal spores in the observations. That means that the improvement noted in summertime in simulated PM10 from the different experiments over background Europe stations for example as shown in Figure 20 could be either a real improvement or compensating some other issues or missing emissions in the model. However, the signal is clearly positive. To go beyond the regions that are often evaluated in CAMS (Europe, US, China), a dataset of air quality from Brazil, which covers the years 2015 to 2022, has been fetched and processed. Figure 21 shows simulated and observed PM10 over Brazil in a summer month (January 2017, summer in S Hemisphere). The impact of the simulated fungal spores is larger over the Amazon and adjacent regions, but most of Brazil is impacted. It is however quite hard to conclude on whether the implementation of a fungal spores species improves simulated PM10 over Brazil.

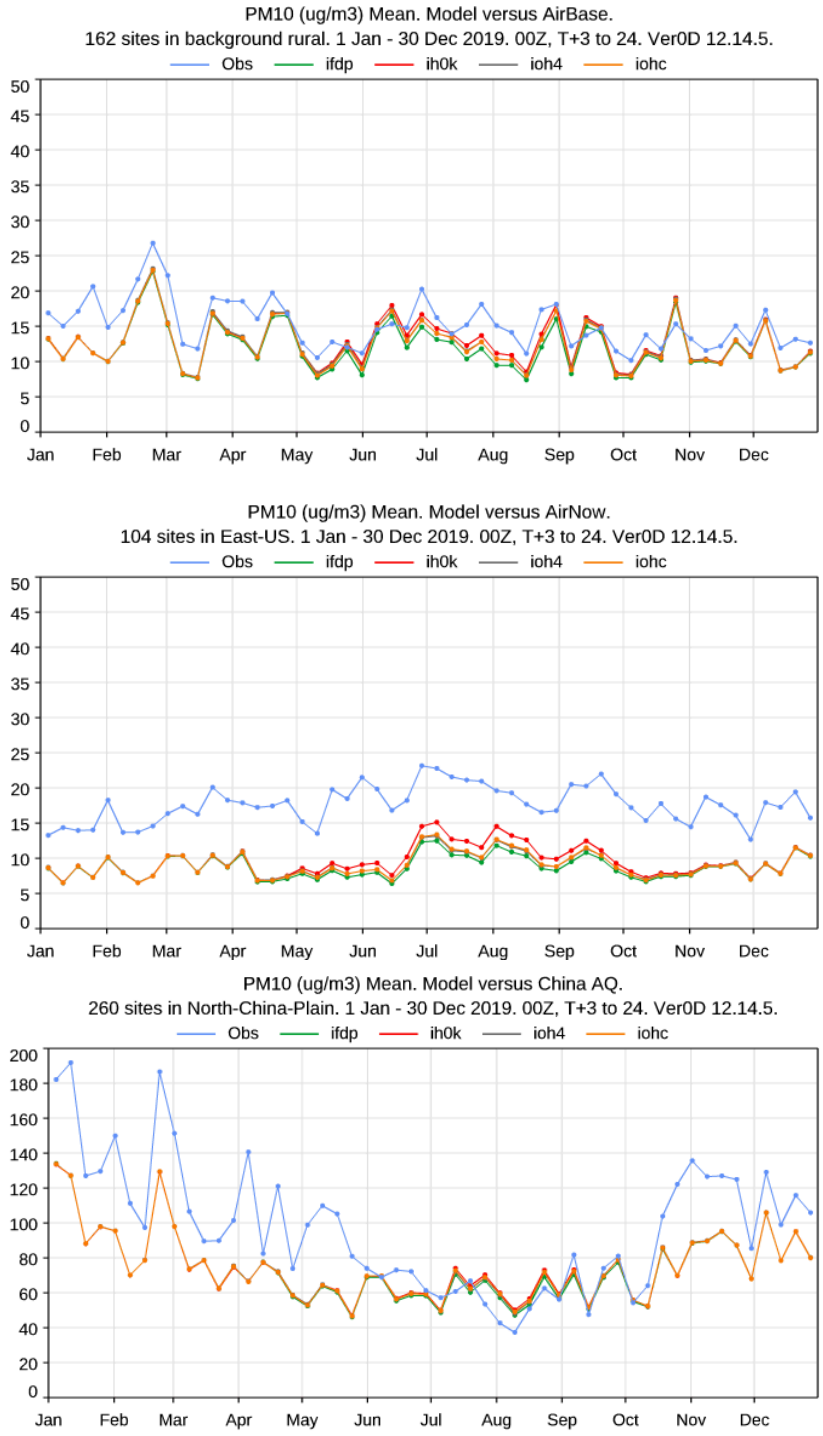

Figure 20. 2019, observed (blue line) and simulated weekly PM10 over European background rural stations (top), East U.S. stations (middle) and North China Plain stations (bottom). **Green is no fungal spores**, **red is HS09**, **orange is H15 adjusted**, **gray is J21 adjusted.**

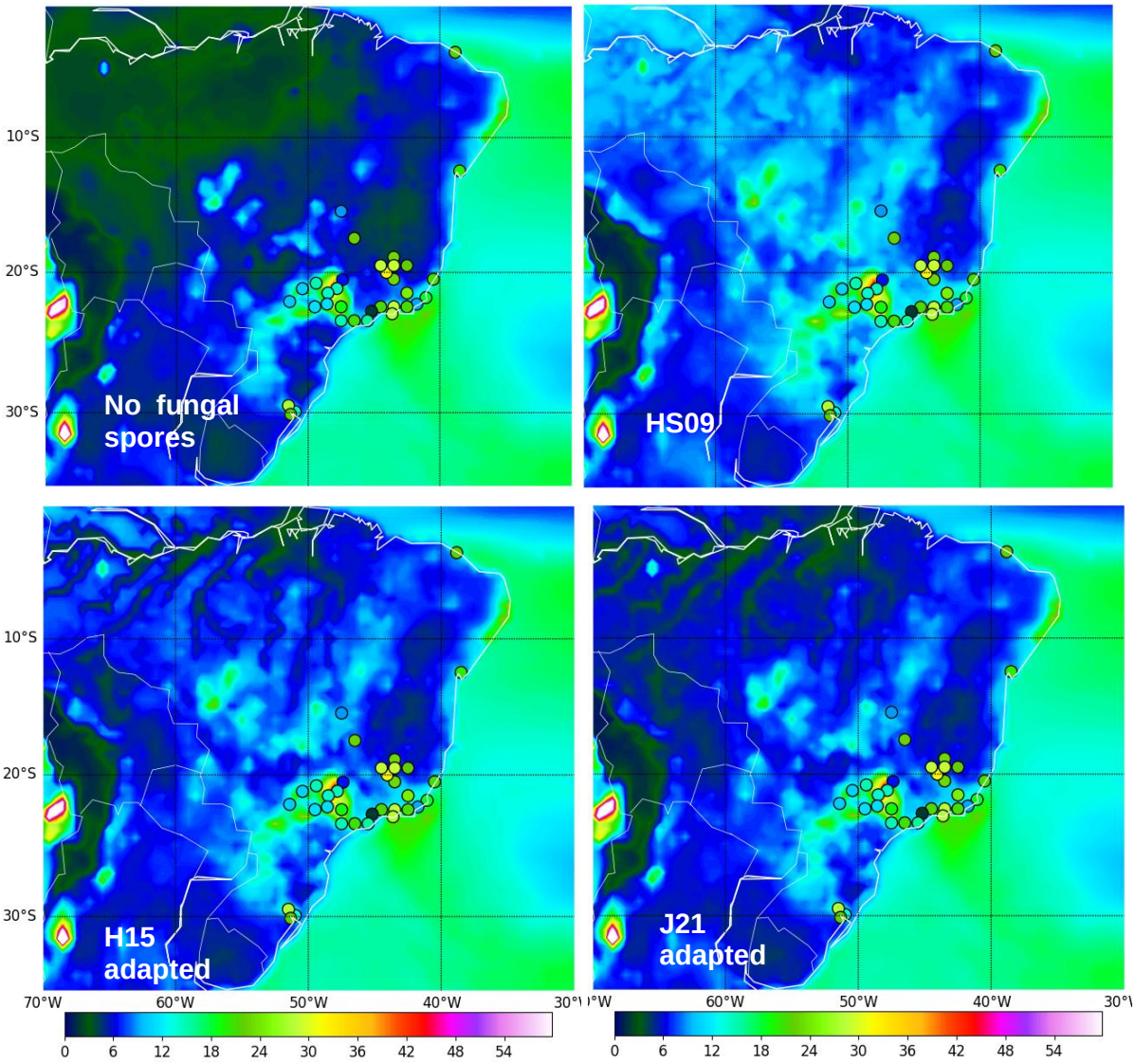

Figure 21. January 2017, observed (circles) and simulated PM10, in µg/m^3. Simulation with no fungal spores (top left); HS09 (top right); adapted H15 (bottom left) and adapted J21 (bottom right).

6.4.4 Single scattering albedo

The impact of fungal spores on simulated aerosol optical depth (AOD) is negligible and thus not shown. However, the implementation of fungal spores has a non negligible impact on simulated single scattering albedo (SSA) and as a consequence on absorption AOD. This is shown in Figure 22, which compares retrieved SSA at 1020nm from AERONET inversion products, as compared against simulated values for simulations without fungal spores and the HS09 experiment, in July 2019. The simulated SSA is lower with HS09, between 0.92 and 0.96 over most of Europe, while for the simulation without fungal spores, the simulated SSA is above 0.95. Over a majority of AERONET stations, this helps in reducing a high bias in simulated SSA at 1020nm. However, as for PM10, this bias reduction could be genuine, or compensating for other issues, such as in the optics used for absorbing species (OM, BC, SOA) or the simulated abundance of these species.

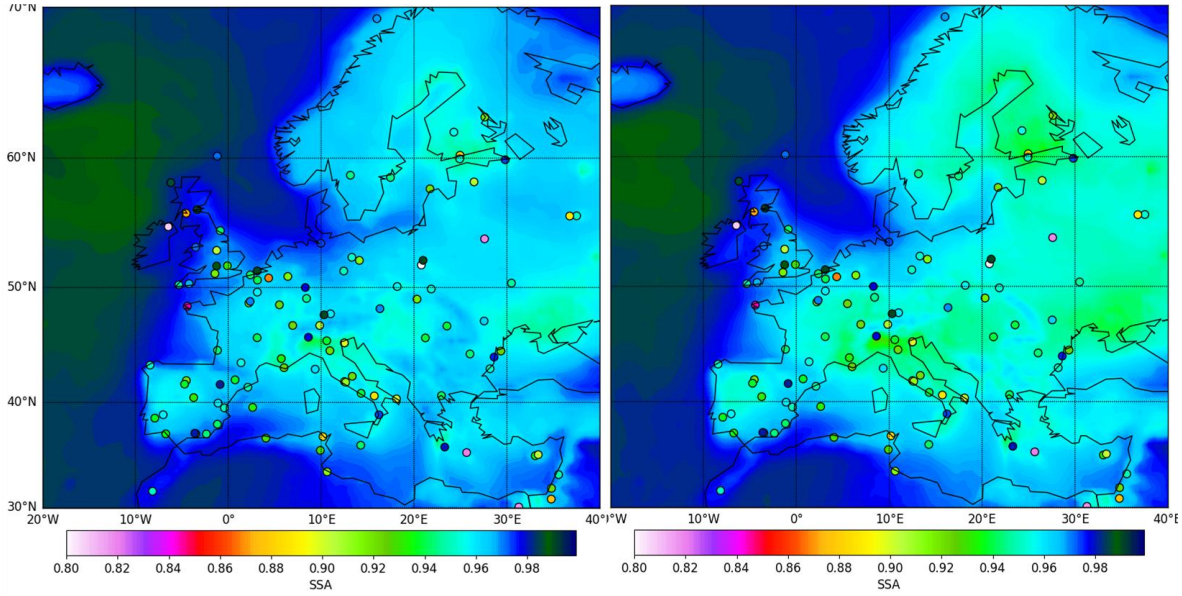

Figure 22. July 2019, observed single scattering albedo at 1020nm from AERONET inversion level 2.0 (circles) against simulated values by a simulation with no fungal spores (left) and HS09 (right).

7 Model intercomparison for fungal spores

In this section, simulated values by IFS-COMPO and EMEP are compared, and also including simulated values by the CHIMERE model as reported in Vida et al (2024). The CHIMERE model also uses the Heald and Spracklen (2009) fungal spores emission scheme. In this section, only the sugar alcohol (arabitol + mannitol) observational data is used.

7.1 A note on data coverage

A common requirement used in EMEP is a 75% coverage rate of data (e.g. at least 21 daily data points for monthly averages). As the arabitol and mannitol data prvided by IGE is available at varying time intervals, and fairly sparsely, we instead include all data in the comparison below. As such, for some stations the monthly averages shown below do not include many days of a month.

7.2 Comparison of time series

The time series for all stations for the year 2017 and 2019 are shown in Fig. 23.

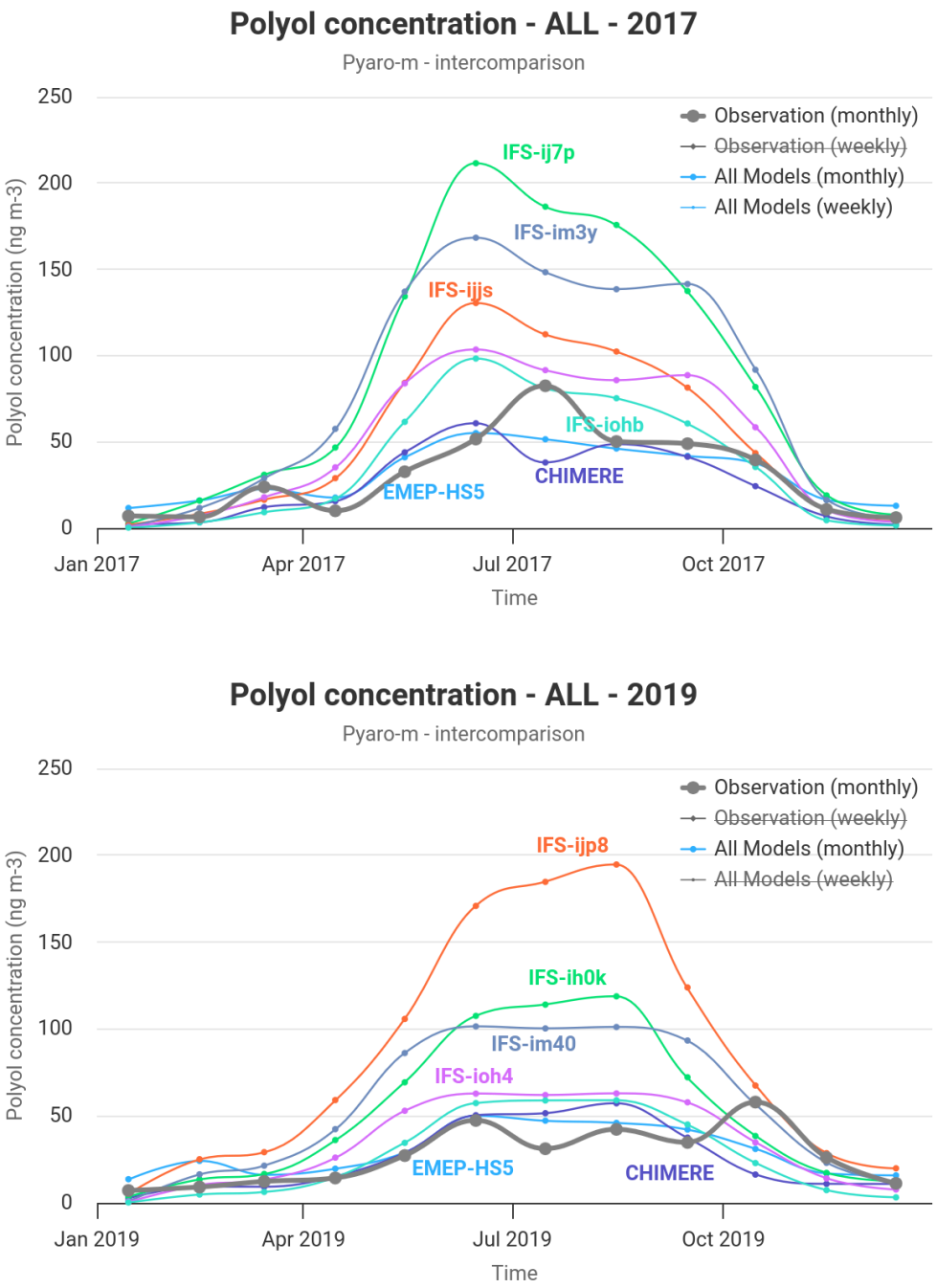

Figure 23. Time series averaged over all stations for 2017 and 2019, comparing various IFS-COMPO parameterizations with the EMEP and CHIMERE parameterizations. For the IFS-COMPO simulations, green is HS09, **orange (IFS-ijjs and ijp8) is H15**, **greenish-blue (IFS-iohb and iohc) is H15 adjusted**, **dark blue (IFS-im3y and im40) is J21** and **violet (IFS-ioh3 and ioh4) is J21 adjusted**.

As can be seen in Figure 23, the IFS-COMPO simulations models are generally significantly higher than both CHIMERE and EMEP. This agrees with the results from Section 5 for EMEP and 6 for IFS-COMPO, that the other parameterizations tend to severely overestimate fungal spores. An additional factor playing into this is that the key inputs of the different parameterizations, and in particular LAI, may differ between IFS-COMPO and the other two models.

Looking at country resolved results, a different pattern emerges as can seen in Figure 24.

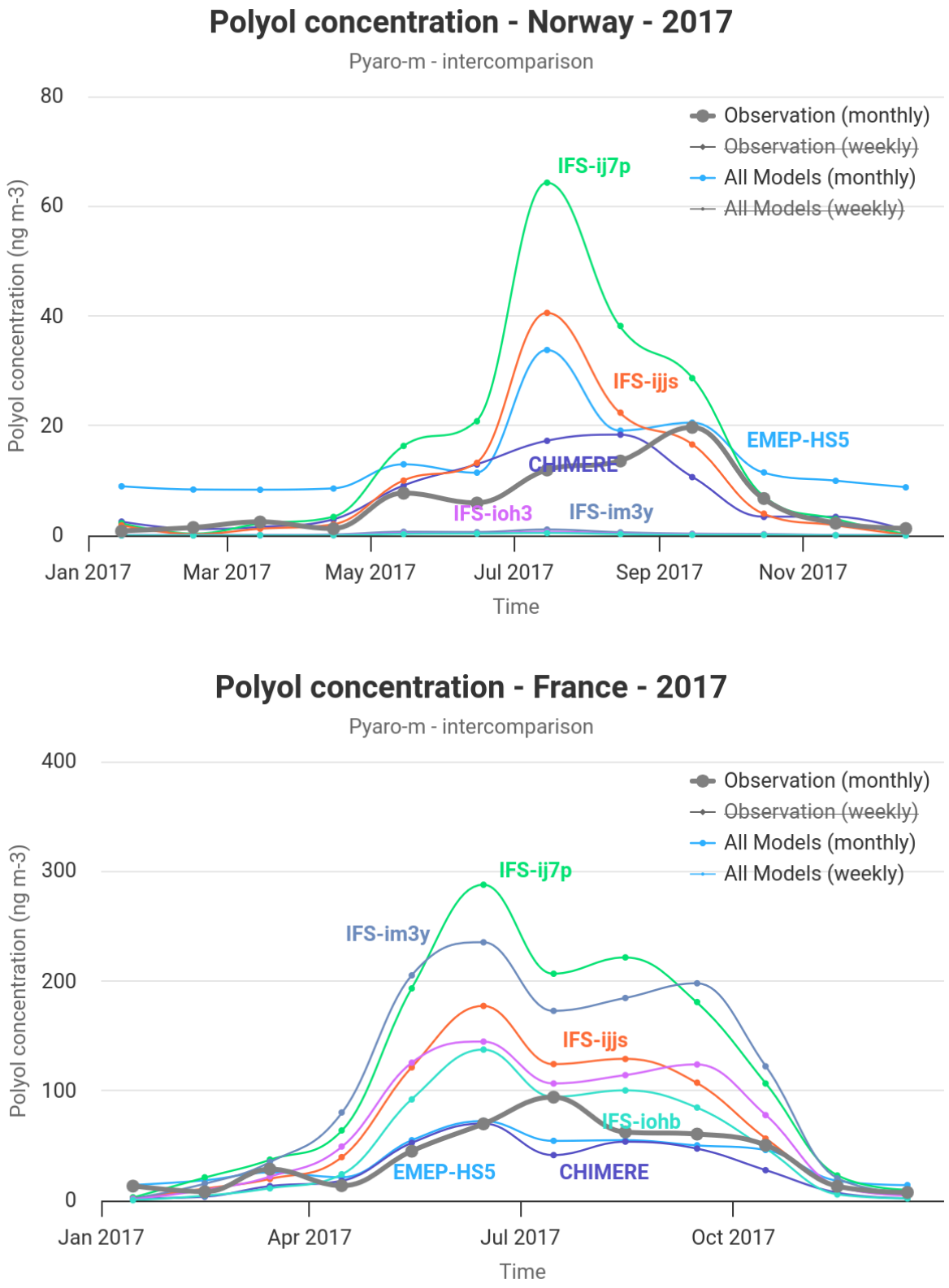

Figure 24: Time series for 2017 for Norwegian and French stations. For the IFS-COMPO simulations, green is HS09, **orange (IFS-ijjs) is H15**, **greenish-blue (IFS-iohb) is H15 adjusted**, **dark blue (IFS-im3y) is J21** and **violet (IFS-ioh3) is J21 adjusted**.

As can be seen in Figure 24, EMEP is significantly worse in Norway compared to France, CHIMERE is somewhat worse, whereas some of the IFS-COMPO simulations are actually slightly better in France.

7.3 Comparison of statistics

To make the qualitative conclusions from the previous section more quantitative, we now compare tThe relevant statistics, including bias and correlation, for the various models. The results are summarized in Figure 25.

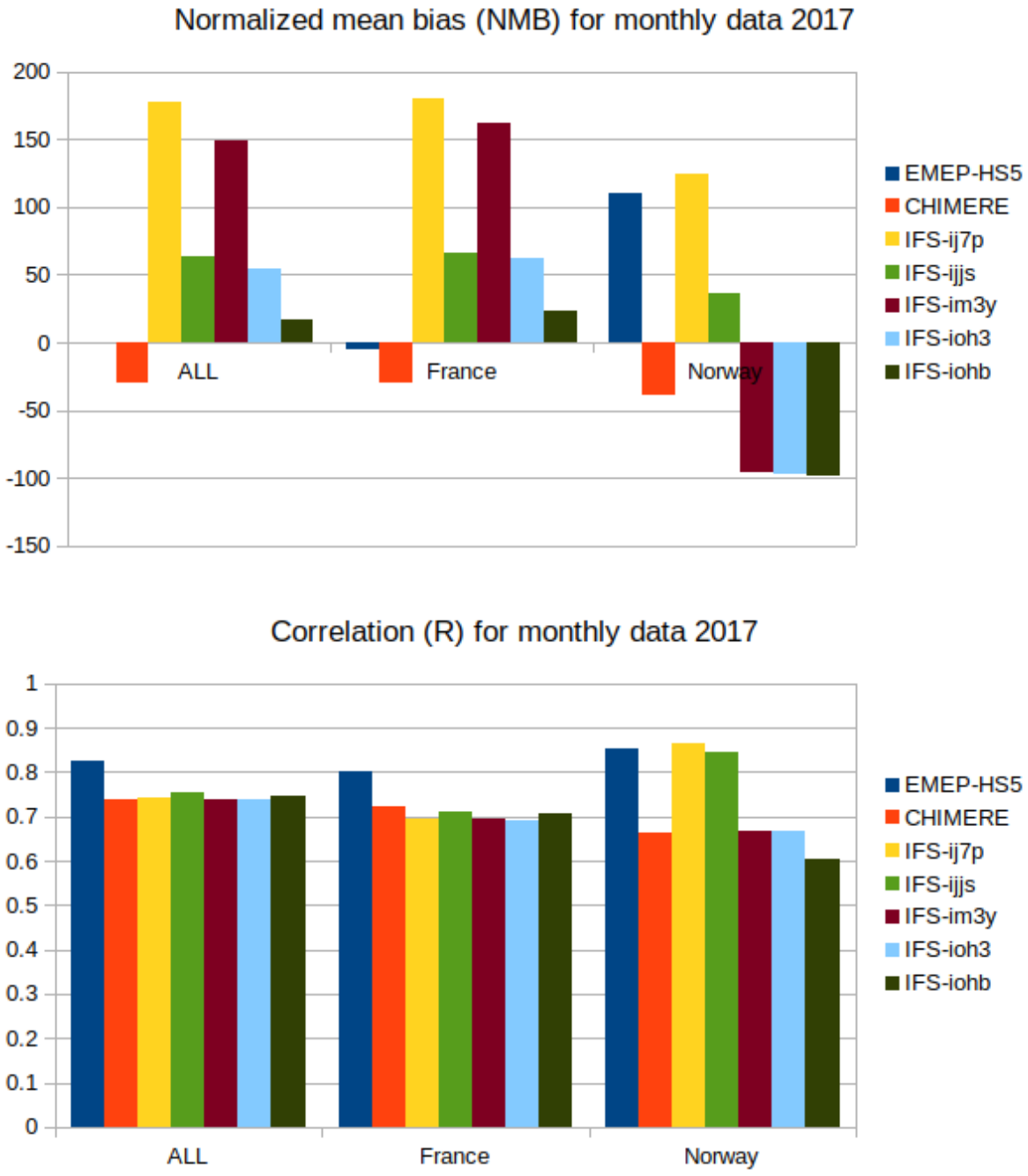

Figure 25: Bias and correlation for the various models compared in this report

As shown above, the EMEP model has the highest overall correlation, and best correlation in France, whereas the IFS-ij7p (HS09) model has a slightly better correlation in Norway. Similarly, the bias magnitude is smallest for EMEP, though there are clearly compensating errors from Norway and France. Note that because there are significantly more observations in France, the extra bias from Norway plays a comparatively smaller role.

For the IFS-COMPO models, the smallest overall bias is found for IFS-iohb, which corresponds to a modified fit from Hummel et al (2015). We note, however, that this is mostly driven by the model working well in France: both the bias and the correlation of this parameterization are quite poor compared to the other parameterization over Norway. The very low simulated values with the adjusted IFS-COMPO experiments as well as J21 (im3y) are caused by issues in the treatment of fungal spores emissions in grid cells that include ocean and land.

Interestingly, the CHIMERE model has a negative bias in all countries, despite nominally using the same emission scheme. This points to systematic differences between the two models, which are of interest to explore further.

7.4 Discussion : impact of Leaf Area Index (LAI)

All parameterizations tested in IFS-COMPO, CHIMERE and EMEP rely on LAI which the key input for fungal spores emissions. However, as discussed in more detail deliverable 7.1 and 5.4 several sources exist for LAI which give quite different results. For example, Figure 26 compares the LAI from low and high vegetation in IFS-COMPO, which are provided by the European Space Agence (ESA) Climate Change Initiative (CCI), which is compute from a synergy of remote sensing information, and LAI computed from the LPJ-GUESS (Lund-Potsdam-Jena General Ecosystem Simulator) vegetation model. LPJ-GUESS is a process-based dynamic vegetation-terrestrial ecosystem model designed for regional or global studies. Given data on regional climate conditions and atmospheric carbon dioxide concentrations, it can predict structural, compositional and functional properties of the native ecosystems of major climate zones of the Earth. Many differences are visible, such as the significantly higher LAI over much of Europe and extra tropical forested areas, in July 2017, with IFS-COMPO LAI. In wintertime, on the hand, IFS-COMPO LAI is generally lower over the same areas. LAI is thus a major source of uncertainties; future work should emphasize on using the work carried out in other deliverables on the adequate use of LAI in global atmospheric composition models.

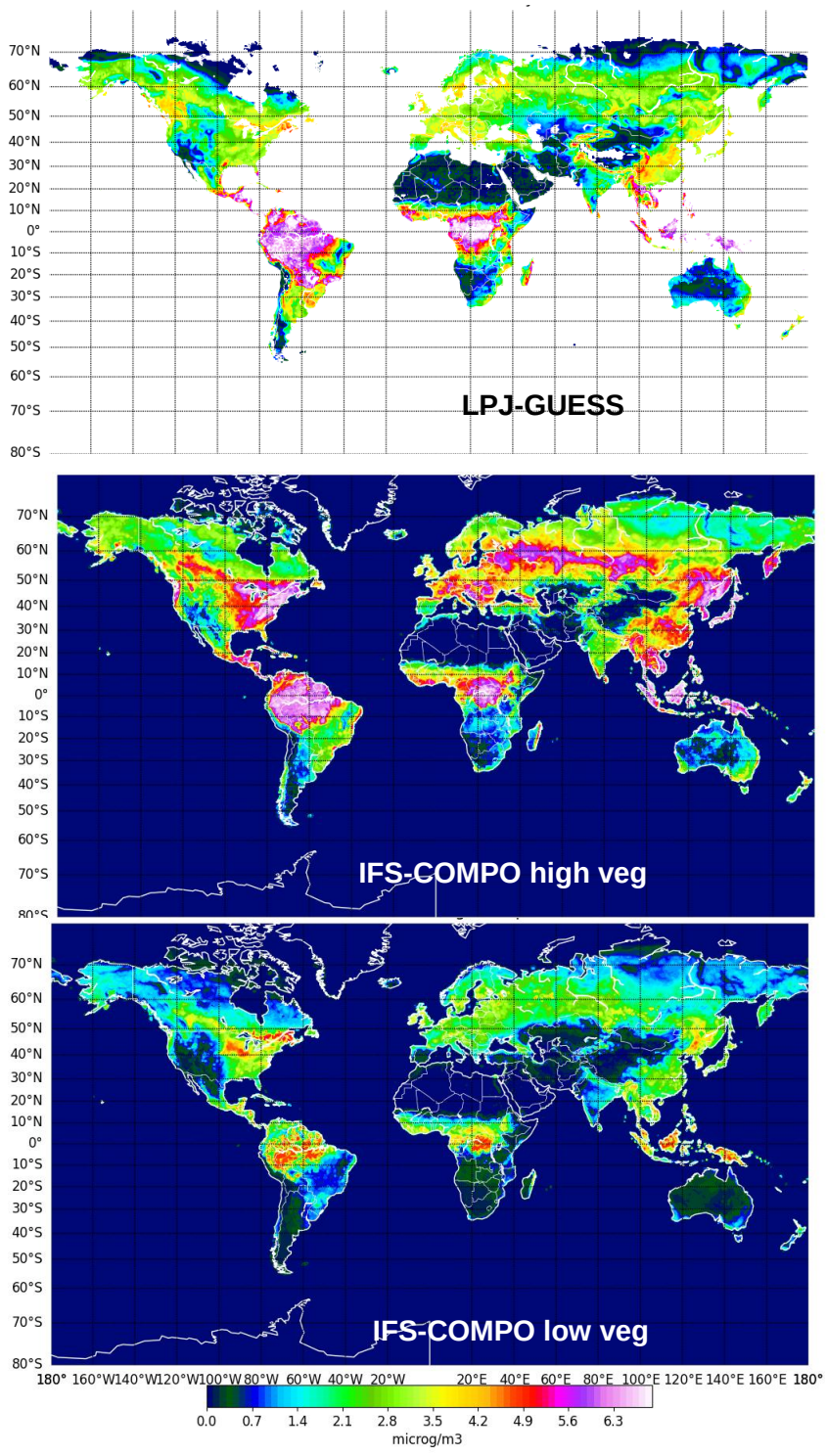

Figure 26: July 2017 LAI from LPJ-GUESS (top), and from IFS-COMPO, high vegetation (middle) and low vegetation (bottom).

7.5 Conclusion of the intercomparison

Fungal spore parameterizations have been implemented in two separate air quality models, and have been compared to both observational data and a third model. The results show a significant dependence on parameterization, suggesting that choosing the correct parameterization is crucial to get an accurate representation of fungal spores.

The existing parameterizations have largely been fitted to small geographic regions, and it is therefore not clear how representative they are over all of Europe or the globe. Furthermore, the parameterizations are heuristic, and do not accurately capture the complex morphology, or the large variety within the fungi kingdom. Given this background, the accuracy of the models (with correlations R>0.7 for most models) is quite decent.

Whilst attempts have been made to improve the parameterization, within both EMEP and IFS-COMPO, ultimately these attempts are hampered by the lack of available data, and the small geographic spread. Efforts are ongoing to acquire additional data, which will make it possible to improve the parameterizations. Possible improvements could be to include biological activity, rather than leaf-area index, as an indicator for fungi growth, and to more deliberately include snow cover and temperature cut-offs, as has already been attempted in EMEP and IFS-COMPO.

Finally, it is of great interest to investigate the significant discrepancies between EMEP/IFS-COMPO and CHIMERE, particularly for the HS-5 parameterization.

8 Conclusion

A new fungal spores lumped species, meant to represent all the diversity of a large number of fungal spores species, has been implemented in EMEP and IFS-COMPO. Several emission parameterizations have been tested and implemented, which use in different ways the same inputs : temperature, specific humidity, leaf area index (LAI) and friction velocity (for the Janssen et al 2021 statistical fit). Different aspects of the simulated fungal spores have been evaluated against a wide range of datasets which has been retrieved after an extensive search, as fungal spores observations are not easy to find in general. It was found that most of the schemes are able to simulated the broad lines of the seasonal cycle. However, some features such as a frequent peak in emissions and surface concentration in the Autumn are not well represented. The impact on PM10 is small but positive in summertime. Overall, despite some issues associated with the representation of a variety of species with a single tracer, and too simple emission schemes, the implementation of a fungal spores species could be a useful addition to the CAMS product portfolio. The EMEP and IFS-COMPO implementations are close to be mature enough for an operational implementation in CAMS.

Future work on fungal spores should focus on the inputs and particularly on LAI, and on the possibility of using other vegetation information, or lagged information such as LAI from ten days ago, as done for the recently implemented IFS-COMPO online BVOC emission module.

9 References

Chapter 7 of the 2024 EMEP report, available at: https://www.emep.int/publ/common_publications.html

Ahlm, L., Krejci, R., Nilsson, E. D., Mårtensson, E. M., Vogt, M., and Artaxo, P.: Emission and dry deposition of accumulation mode particles in the Amazon Basin, Atmos. Chem. Phys., 10, 10237–10253, https://doi.org/10.5194/acp-10-10237-2010, 2010.

Bakwin, P. S., Davis, K. J., Yi, C., Wofsy, S. C., Munger, J. W., Haszpra, L., and Barcza, Z.: Regional carbon dioxide fluxes from mixing ratio data, Tellus B, 56, 301–311, https://doi.org/10.1111/j.1600-0889.2004.00111.x, 2004.

Bauer, H., Schueller, E., Weinke, G., Berger, A., Hitzenberger, R., Marr, I. L., and Puxbaum, H.: Significant contributions of fungal spores to the organic carbon and to the aerosol mass balance of the urban atmospheric aerosol, Atmospheric Environment, 42, 5542–5549, 2008.

Behrenfeld, M. J., Moore, R. H., Hostetler, C. A., Graff, J., Gaube, P., Russell, L. M., Chen, G., Doney, S. C., Giovannoni, S., Liu, H., Proctor, C., Bolaños, L. M., Baetge, N., Davie-Martin, C., Westberry, T. K., Bates, T. S., Bell, T. G., Bidle, K. D., Boss, E. S., Brooks, S. D., Cairns, B., Carlson, C., Halsey, K., Harvey, E. L., Hu, C., Karp-Boss, L., Kleb, M., Menden-Deuer, S., Morison, F., Quinn, P. K., Scarino, A. J., Anderson, B., Chowdhary, J., Crosbie, E., Ferrare, R., Hair, J. W., Hu, Y., Janz, S., Redemann, J., Saltzman, E., Shook, M., Siegel, D. A., Wisthaler, A., Martin, M. Y., and Ziemba, L.: The North Atlantic Aerosol and Marine Ecosystem Study (NAAMES): Science Motive and Mission Overview, Front. Mar. Sci., 6, 122, https://doi.org/10.3389/fmars.2019.00122, 2019.

Betts, A. K.: Idealized Model for Equilibrium Boundary Layer over Land, J. Hydrometeorol., 1, 507–523, https://doi.org/10.1175/1525-7541(2000)001<0507:IMFEBL>2.0.CO;2, 2000.

Boddy, L., Büntgen, U., Egli, S., Gange, A. C., Heegaard, E., Kirk, P. M., Mohammad, A., and Kauserud, H.: Climate variation effects on fungal fruiting, Fungal Ecol., 10, 20–33, https://doi.org/10.1016/j.funeco.2013.10.006, 2014.

Burrows, S. M., Butler, T., Jöckel, P., Tost, H., Kerkweg, A., Pöschl, U., and Lawrence, M. G.: Bacteria in the global atmosphere – Part 2: Modeling of emissions and transport between different ecosystems, Atmos. Chem. Phys., 9, 9281–9297, https://doi.org/10.5194/acp-9-9281-2009, 2009.

Carotenuto, F., Georgiadis, T., Gioli, B., Leyronas, C., Morris, C. E., Nardino, M., Wohlfahrt, G., and Miglietta, F.: Measurements and modeling of surface–atmosphere exchange of microorganisms in Mediterranean grassland, Atmos. Chem. Phys., 17, 14919–14936, https://doi.org/10.5194/acp-17-14919-2017, 2017.

China, S., Wang, B., Weis, J., Rizzo, L., Brito, J., Cirino, G. G., Kovarik, L., Artaxo, P., Gilles, M. K., and Laskin, A.: Rupturing of biological spores as a source of secondary particles in Amazonia, Environ. Sci. Technol., 50, 12179–12186, https://doi.org/10.1021/acs.est.6b02896, 2016.

China, S., Burrows, S. M., Wang, B., Harder, T. H., Weis, J., Tanarhte, M., Rizzo, L. V., Brito, J., Cirino, G. G., Ma, P.-L., Cliff, J., Artaxo, P., Gilles, M. K., and Laskin, A.: Fungal spores as a source of sodium salt particles in the Amazon basin, Nat. Commun., 9, 4793, https://doi.org/10.1038/s41467-018-07066-4, 2018.

Crawford, I., Robinson, N. H., Flynn, M. J., Foot, V. E., Gallagher, M. W., Huffman, J. A., Stanley, W. R., and Kaye, P. H.: Characterisation of bioaerosol emissions from a Colorado pine forest: results from the BEACHON-RoMBAS experiment, Atmos. Chem. Phys., 14, 8559–8578, https://doi.org/10.5194/acp-14-8559-2014, 2014.

Crawford, I., Ruske, S., Topping, D. O., and Gallagher, M. W.: Evaluation of hierarchical agglomerative cluster analysis methods for discrimination of primary biological aerosol, Atmos. Meas. Tech., 8, 4979–4991, https://doi.org/10.5194/amt-8-4979-2015, 2015.

Damialis, A., Mohammad, A. B., Halley, J. M., and Gange, A. C.: Fungi in a changing world: growth rates will be elevated, but spore production may decrease in future climates, Int. J. Biometeorol., 59, 1157–1167, https://doi.org/10.1007/s00484-014-0927-0, 2015.

DeLeon-Rodriguez, N., Lathem, T. L., Rodriguez, L. M., Barazesh, J. M., Anderson, B. E., Beyersdorf, A. J., Ziemba, L. D., Bergin, M., Nenes, A., and Konstantinidis, K. T.: Microbiome of the upper troposphere: Species composition and prevalence, effects of tropical storms, and atmospheric implications, P. Natl. Acad. Sci. USA, 110, 2575–2580, https://doi.org/10.1073/pnas.1212089110, 2013.

Després, V., Huffman, J., Burrows, S., Hoose, C., Safatov, A., Buryak, G., Fröhlich-Nowoisky, J., Elbert, W., Andreae, M., Pöschl, U., and Ruprecht, J.: Primary biological aerosol particles in the atmosphere: a review, Tellus B, 64, 15598 https://doi.org/10.3402/tellusb.v64i0.15598, 2012.

Elbert, W., Taylor, P. E., Andreae, M. O., and Pöschl, U.: Contribution of fungi to primary biogenic aerosols in the atmosphere: wet and dry discharged spores, carbohydrates, and inorganic ions, Atmos. Chem. Phys., 7, 4569–4588, https://doi.org/10.5194/acp-7-4569-2007, 2007.

Fisher, M. C., Henk, D. A., Briggs, C. J., Brownstein, J. S., Madoff, L. C., McCraw, S. L., and Gurr, S. J.: Emerging fungal threats to animal, plant and ecosystem health, Nature, 484, 186–194, https://doi.org/10.1038/nature10947, 2012.

Fröhlich-Nowoisky, J., Kampf, C. J., Weber, B., Huffman, J. A., Pöhlker, C., Andreae, M. O., Lang-Yona, N., Burrows, S. M., Gunthe, S. S., Elbert, W., Su, H., Hoor, P., Thines, E., Hoffmann, T., Desprès, V. R., and Pöschl, U.: Bioaerosols in the Earth system: Climate, health, and ecosystem interactions, Atmos. Res., 182, 346–376, https://doi.org/10.1016/j.atmosres.2016.07.018, 2016.

Gabey, A. M., Gallagher, M. W., Whitehead, J., Dorsey, J. R., Kaye, P. H., and Stanley, W. R.: Measurements and comparison of primary biological aerosol above and below a tropical forest canopy using a dual channel fluorescence spectrometer, Atmos. Chem. Phys., 10, 4453–4466, https://doi.org/10.5194/acp-10-4453-2010, 2010.

Gange, A. C., Gange, E. G., Sparks, T. H., and Boddy, L.: Rapid and Recent Changes in Fungal Fruiting Patterns, Science, 316, p. 71, https://doi.org/10.1126/science.1137489, 2007.

Geagea, L., Huber, L., Sache, I., Flura, D., McCartney, H. A., and Fitt, B. D. L.: Influence of simulated rain on dispersal of rust spores from infected wheat seedlings, Agr. Forest Meteorol., 101, 53–66, https://doi.org/10.1016/S0168-1923(99)00155-0, 2000.

Gelaro, R., McCarty, W., Suárez, M. J., Todling, R., Molod, A., Takacs, L., Randles, C. A., Darmenov, A., Bosilovich, M. G., Reichle, R., Wargan, K., Coy, L., Cullather, R., Draper, C., Akella, S., Buchard, V., Conaty, A., da Silva, A. M., Gu, W., Kim, G.-K., Koster, R., Lucchesi, R., Merkova, D., Nielsen, J. E., Partyka, G., Pawson, S., Putman, W., Rienecker, M., Schubert, S. D., Sienkiewicz, M., and Zhao, B.: The Modern-Era Retrospective Analysis for Research and Applications, Version 2 (MERRA-2), J. Climate, 30, 5419–5454, https://doi.org/10.1175/JCLI-D-16-0758.1, 2017.

Haga, D. I., Burrows, S. M., Iannone, R., Wheeler, M. J., Mason, R. H., Chen, J., Polishchuk, E. A., Pöschl, U., and Bertram, A. K.: Ice nucleation by fungal spores from the classes *Agaricomycetes*, *Ustilaginomycetes*, and *Eurotiomycetes*, and the effect on the atmospheric transport of these spores, Atmos. Chem. Phys., 14, 8611–8630, https://doi.org/10.5194/acp-14-8611-2014, 2014.

Heald, C. L. and Spracklen, D. V.: Atmospheric budget of primary biological aerosol particles from fungal spores, Geophys. Res. Lett., 36, L09806, https://doi.org/10.1029/2009GL037493, 2009.

Helliker, B. R., Berry, J. A., Betts, A. K., Bakwin, P. A., Davis, K., Denning, A. S., Ehleringer, J. R., Miller, J. B., Butler, M. B., and Ricciuto, D. M.: Estimates of net CO_2 flux by application of equilibrium boundary layer concepts to CO_2 and water vapor measurements from a tall tower, J. Geophys. Res., 109, D20106, https://doi.org/10.1029/2004JD004532, 2004.

Hirst, J. M.: An Automatic Volumetric Spore Trap, Ann. Appl. Biol., 39, 257–265, https://doi.org/10.1111/j.1744-7348.1952.tb00904.x, 1952.

Hoose, C., Kristjánsson, J. E., and Burrows, S. M.: How important is biological ice nucleation in clouds on a global scale?, Environ. Res. Lett., 5, 024009, https://doi.org/10.1088/1748-9326/5/2/024009, 2010.

Huffman, J. A., Sinha, B., Garland, R. M., Snee-Pollmann, A., Gunthe, S. S., Artaxo, P., Martin, S. T., Andreae, M. O., and Pöschl, U.: Size distributions and temporal variations of biological aerosol particles in the Amazon rainforest characterized by microscopy and real-time UV-APS fluorescence techniques during AMAZE-08, Atmos. Chem. Phys., 12, 11997–12019, https://doi.org/10.5194/acp-12-11997-2012, 2012.

Huffman, J. A., Prenni, A. J., DeMott, P. J., Pöhlker, C., Mason, R. H., Robinson, N. H., Fröhlich-Nowoisky, J., Tobo, Y., Després, V. R., Garcia, E., Gochis, D. J., Harris, E., Müller-Germann, I., Ruzene, C., Schmer, B., Sinha, B., Day, D. A., Andreae, M. O., Jimenez, J. L., Gallagher, M., Kreidenweis, S. M., Bertram, A. K., and Pöschl, U.: High concentrations of biological aerosol particles and ice nuclei during and after rain, Atmos. Chem. Phys., 13, 6151–6164, https://doi.org/10.5194/acp-13-6151-2013, 2013.

Huffman, J. A., Perring, A. E., Savage, N. J., Clot, B., Crouzy, B., Tummon, F., Shoshanim, O., Damit, B., Schneider, J., Sivaprakasam, V., Zawadowicz, M. A., Crawford, I., Gallagher, M., Topping, D., Doughty, D. C., Hill, S. C., and Pan, Y.: Real-time sensing of bioaerosols: Review and current perspectives, Aerosol Sci. Technol., 54, 465–495, https://doi.org/10.1080/02786826.2019.1664724, 2020.

Hummel, M., Hoose, C., Gallagher, M., Healy, D. A., Huffman, J. A., O'Connor, D., Pöschl, U., Pöhlker, C., Robinson, N. H., Schnaiter, M., Sodeau, J. R., Stengel, M., Toprak, E., and Vogel, H.: Regional-scale simulations of fungal spore aerosols using an emission parameterization adapted to local measurements of fluorescent biological aerosol particles, Atmos. Chem. Phys., 15, 6127–6146, https://doi.org/10.5194/acp-15-6127-2015, 2015.

Jacobson, M. Z. and Streets, D. G.: Influence of future anthropogenic emissions on climate, natural emissions, and air quality, J. Geophys. Res.-Atmos., 114, D08118, https://doi.org/10.1029/2008JD011476, 2009.

Jaenicke, R.: Abundance of Cellular Material and Proteins in the Atmosphere, Science, 308, 73–73, https://doi.org/10.1126/science.1106335, 2005.

Jones, A. M. and Harrison, R. M.: The effects of meteorological factors on atmospheric bioaerosol concentrations – a review, Sci. Total Environ., 326, 151–180, https://doi.org/10.1016/j.scitotenv.2003.11.021, 2004.

Kauserud, H., Stige, L. C., Vik, J. O., Økland, R. H., Høiland, K., and Stenseth, N. Chr.: Mushroom fruiting and climate change, P. Natl. Acad. Sci. USA, 105, 3811–3814, https://doi.org/10.1073/pnas.0709037105, 2008.

Keller, C. A., Long, M. S., Yantosca, R. M., Da Silva, A. M., Pawson, S., and Jacob, D. J.: HEMCO v1.0: a versatile, ESMF-compliant component for calculating emissions in atmospheric models, Geosci. Model Dev., 7, 1409–1417, https://doi.org/10.5194/gmd-7-1409-2014, 2014.

Lawler, M. J., Draper, D. C., and Smith, J. N.: Atmospheric fungal nanoparticle bursts, Sci. Adv., 6, eaax9051, https://doi.org/10.1126/sciadv.aax9051, 2020.

Levetin, E.: Methods for aeroallergen sampling, Curr. Allergy Asthma R., 4, 376–383, https://doi.org/10.1007/s11882-004-0088-z, 2004.

Liu, H., Jacob, D. J., Bey, I., and Yantosca, R. M.: Constraints from 210Pb and 7Be on wet deposition and transport in a global three-dimensional chemical tracer model driven by assimilated meteorological fields, J. Geophys. Res.-Atmos., 106, 12109–12128, https://doi.org/10.1029/2000JD900839, 2001.

Löbs, N., Barbosa, C. G. G., Brill, S., Walter, D., Ditas, F., de Oliveira Sá, M., de Araújo, A. C., de Oliveira, L. R., Godoi, R. H. M., Wolff, S., Piepenbring, M., Kesselmeier, J., Artaxo, P., Andreae, M. O., Pöschl, U., Pöhlker, C., and Weber, B.: Aerosol measurement methods to quantify spore emissions from fungi and cryptogamic covers in the Amazon, Atmos. Meas. Tech., 13, 153–164, https://doi.org/10.5194/amt-13-153-2020, 2020.

Manninen, H. E., Sihto-Nissilä, S.-L., Hiltunen, V., Aalto, P. P., Kulmala, M., Petäjä, T., Manninen, H. E., Bäck, J., Hari, P., Huffman, J. A., Huffman, J. A., Saarto, A., Pessi, A.-M., and Hidalgo, P. J.: Patterns in airborne pollen and other primary biological aerosol particles (PBAP), and their contribution to aerosol mass and number in a boreal forest, Boreal Environ. Res., 19, 383–405, 2014.

McNaughton, C. S., Clarke, A. D., Howell, S. G., Pinkerton, M., Anderson, B., Thornhill, L., Hudgins, C., Winstead, E., Dibb, J. E., Scheuer, E., and Maring, H.: Results from the DC-8 Inlet Characterization Experiment (DICE): Airborne Versus Surface Sampling of Mineral Dust and Sea Salt Aerosols, Aerosol Sci. Technol., 41, 136–159, https://doi.org/10.1080/02786820601118406, 2007.

Mesinger, F., DiMego, G., Kalnay, E., Mitchell, K., Shafran, P. C., Ebisuzaki, W., Jović, D., Woollen, J., Rogers, E., Berbery, E. H., Ek, M. B., Fan, Y., Grumbine, R., Higgins, W., Li, H., Lin, Y., Manikin, G., Parrish, D., and Shi, W.: North American Regional Reanalysis, B. Am. Meteorol. Soc., 87, 343–360, https://doi.org/10.1175/BAMS-87-3-343, 2006.

Morris, C. E., Conen, F., Alex Huffman, J., Phillips, V., Pöschl, U., and Sands, D. C.: Bioprecipitation: a feedback cycle linking Earth history, ecosystem dynamics and land use through biological ice nucleators in the atmosphere, Glob. Change Biol., 20, 341–351, https://doi.org/10.1111/gcb.12447, 2014.

Myneni, R. B., Knyazikhin, Y., and Park, T.: MCD15A3H MODIS/Terra+Aqua Leaf Area Index/FPAR 4-day L4 Global 500m SIN Grid V006, distributed by NASA EOSDIS Land Processes DAAC, https://doi.org/10.5067/MODIS/MCD15A3H.006, 2015.

Myriokefalitakis, S., Fanourgakis, G., and Kanakidou, M.: The Contribution of Bioaerosols to the Organic Carbon Budget of the Atmosphere, in: Perspectives on Atmospheric Sciences, edited by: Karacostas, T., Bais, A., and Nastos, P. T., Springer International Publishing, Cham, Germany, 845–851, https://doi.org/10.1007/978-3-319-35095-0_121, 2017.

Newville, M., Stensitzki, T., Allen, D. B., and Ingargiola, A.: LMFIT: Non-Linear Least-Square Minimization and Curve-Fitting for Python, Zenodo, https://doi.org/10.5281/zenodo.11813, 2014.

Olson, D. M., Dinerstein, E., Wikramanayake, E. D., Burgess, N. D., Powell, G. V. N., Underwood, E. C., D'amico, J. A., Itoua, I., Strand, H. E., Morrison, J. C., Loucks, C. J., Allnutt, T. F., Ricketts, T. H., Kura, Y., Lamoreux, J. F., Wettengel, W. W., Hedao, P., and Kassem, K. R.: Terrestrial Ecoregions of the World: A New Map of Life on Earth: A new global map of terrestrial ecoregions provides an innovative tool for conserving biodiversity, BioScience, 51, 933–938, https://doi.org/10.1641/0006-3568(2001)051[0933:TEOTWA]2.0.CO;2, 2001.

O'Sullivan, D., Murray, B. J., Ross, J. F., Whale, T. F., Price, H. C., Atkinson, J. D., Umo, N. S., and Webb, M. E.: The relevance of nanoscale biological fragments for ice nucleation in clouds, Sci. Rep., 5, 8082, https://doi.org/10.1038/srep08082, 2015.

Perring, A. E., Schwarz, J. P., Baumgardner, D., Hernandez, M. T., Spracklen, D. V., Heald, C. L., Gao, R. S., Kok, G., McMeeking, G. R., McQuaid, J. B., and Fahey, D. W.: Airborne observations of regional variation in fluorescent aerosol across the United States, J. Geophys. Res.-Atmos., 120, 1153–1170, https://doi.org/10.1002/2014JD022495, 2015.

Porter, W. C., Heald, C. L., Cooley, D., and Russell, B.: Investigating the observed sensitivities of air-quality extremes to meteorological drivers via quantile regression, Atmos. Chem. Phys., 15, 10349–10366, https://doi.org/10.5194/acp-15-10349-2015, 2015.

Pöschl, U., Martin, S. T., Sinha, B., Chen, Q., Gunthe, S. S., Huffman, J. A., Borrmann, S., Farmer, D. K., Garland, R. M., Helas, G., Jimenez, J. L., King, S. M., Manzi, A., Mikhailov, E., Pauliquevis, T., Petters, M. D., Prenni, A. J., Roldin, P., Rose, D., Schneider, J., Su, H., Zorn, S. R., Artaxo, P., and Andreae, M. O.: Rainforest aerosols as biogenic nuclei of clouds and precipitation in the Amazon, Science, 329, 1513–1516, https://doi.org/10.1126/science.1191056, 2010.

Pratt, K. A., DeMott, P. J., French, J. R., Wang, Z., Westphal, D. L., Heymsfield, A. J., Twohy, C. H., Prenni, A. J., and Prather, K. A.: In situ detection of biological particles in cloud ice-crystals, Nat. Geosci., 2, 398–401, https://doi.org/10.1038/ngeo521, 2009.

Prenni, A. J., Petters, M. D., Kreidenweis, S. M., Heald, C. L., Martin, S. T., Artaxo, P., Garland, R. M., Wollny, A. G., and Poschl, U.: Relative roles of biogenic emissions and Saharan dust as ice nuclei in the Amazon basin, Nat. Geosci., 2, 402–405, https://doi.org/10.1038/ngeo517, 2009.

Prenni, A. J., Tobo, Y., Garcia, E., DeMott, P. J., Huffman, J. A., McCluskey, C. S., Kreidenweis, S. M., Prenni, J. E., Pöhlker, C., and Pöschl, U.: The impact of rain on ice nuclei populations at a forested site in Colorado, Geophys. Res. Lett., 40, 227–231, https://doi.org/10.1029/2012GL053953, 2013.

Pringle, A., Patek, S. N., Fischer, M., Stolze, J., and Money, N. P.: The captured launch of a ballistospore, Mycologia, 97, 866–871, https://doi.org/10.1080/15572536.2006.11832777, 2005.

Reinmuth-Selzle, K., Kampf, C. J., Lucas, K., Lang-Yona, N., Fröhlich-Nowoisky, J., Shiraiwa, M., Lakey, P. S. J., Lai, S., Liu, F., Kunert, A. T., Ziegler, K., Shen, F., Sgarbanti, R., Weber, B., Bellinghausen, I., Saloga, J., Weller, M. G., Duschl, A., Schuppan, D., and Pöschl, U.: Air Pollution and Climate Change Effects on Allergies in the Anthropocene: Abundance, Interaction, and Modification of Allergens and Adjuvants, Environ. Sci. Technol., 51, 4119–4141, https://doi.org/10.1021/acs.est.6b04908, 2017.

Samake, A., Uzu, G., Martins, J. M. F., Calas, A., Vince, E., Parat, S., and Jaffrezo, J. L.: The unexpected role of bioaerosols in the Oxidative Potential of PM, Sci. Rep., 7, 10978, https://doi.org/10.1038/s41598-017-11178-0, 2017.

Sarda-Estève, R., Baisnée, D., Guinot, B., Sodeau, J., O'Connor, D., Belmonte, J., Besancenot, J.-P., Petit, J.-E., Thibaudon, M., Oliver, G., Sindt, C., and Gros, V.: Variability and Geographical Origin of Five Years Airborne Fungal Spore Concentrations Measured at Saclay, France from 2014 to 2018, Remote Sens., 11, 1671, https://doi.org/10.3390/rs11141671, 2019.

Savage, N. J., Krentz, C. E., Könemann, T., Han, T. T., Mainelis, G., Pöhlker, C., and Huffman, J. A.: Systematic characterization and fluorescence threshold strategies for the wideband integrated bioaerosol sensor (WIBS) using size-resolved biological and interfering particles, Atmos. Meas. Tech., 10, 4279–4302, https://doi.org/10.5194/amt-10-4279-2017, 2017.

Schumacher, C. J., Pöhlker, C., Aalto, P., Hiltunen, V., Petäjä, T., Kulmala, M., Pöschl, U., and Huffman, J. A.: Seasonal cycles of fluorescent biological aerosol particles in boreal and semi-arid forests of Finland and Colorado, Atmos. Chem. Phys., 13, 11987–12001, https://doi.org/10.5194/acp-13-11987-2013, 2013.

Sesartic, A. and Dallafior, T. N.: Global fungal spore emissions, review and synthesis of literature data, Biogeosciences, 8, 1181–1192, https://doi.org/10.5194/bg-8-1181-2011, 2011.

Silva, S. J. and Heald, C. L.: Investigating Dry Deposition of Ozone to Vegetation, J. Geophys. Res.-Atmos., 123, 559–573, https://doi.org/10.1002/2017JD027278, 2018.

Spracklen, D. V. and Heald, C. L.: The contribution of fungal spores and bacteria to regional and global aerosol number and ice nucleation immersion freezing rates, Atmos. Chem. Phys., 14, 9051–9059, https://doi.org/10.5194/acp-14-9051-2014, 2014.

Steiner, A. L., Brooks, S. D., Deng, C., Thornton, D. C. O., Pendleton, M. W., and Bryant, V.: Pollen as atmospheric cloud condensation nuclei, Geophys. Res. Lett., 42, 3596–3602, https://doi.org/10.1002/2015GL064060, 2015.

Tobo, Y., Prenni, A. J., DeMott, P. J., Huffman, J. A., McCluskey, C. S., Tian, G., Pöhlker, C., Pöschl, U., and Kreidenweis, S. M.: Biological aerosol particles as a key determinant of ice nuclei populations in a forest ecosystem, J. Geophys. Res.-Atmos., 118, 10100–10110, https://doi.org/10.1002/jgrd.50801, 2013.

Toprak, E. and Schnaiter, M.: Fluorescent biological aerosol particles measured with the Waveband Integrated Bioaerosol Sensor WIBS-4: laboratory tests combined with a one year field study, Atmos. Chem. Phys., 13, 225–243, https://doi.org/10.5194/acp-13-225-2013, 2013.

Twohy, C. H., McMeeking, G. R., DeMott, P. J., McCluskey, C. S., Hill, T. C. J., Burrows, S. M., Kulkarni, G. R., Tanarhte, M., Kafle, D. N., and Toohey, D. W.: Abundance of fluorescent biological aerosol particles at temperatures conducive to the formation of mixed-phase and cirrus clouds, Atmos. Chem. Phys., 16, 8205–8225, https://doi.org/10.5194/acp-16-8205-2016, 2016.

Vida, M., Foret, G., Siour, G., Couvidat, F., Favez, O., Uzu, G., Cholakian, A., Conil, S., Beekmann, M., and Jaffrezo, J.-L.: Modelling of atmospheric concentrations of fungal spores: a 2-year simulation over France using CHIMERE, Atmos. Chem. Phys., 24, 10601–10615, https://doi.org/10.5194/acp-24-10601-2024, 2024.

Williams, I. N., Riley, W. J., Torn, M. S., Berry, J. A., and Biraud, S. C.: Using boundary layer equilibrium to reduce uncertainties in transport models and CO_2 flux inversions, Atmos. Chem. Phys., 11, 9631–9641, https://doi.org/10.5194/acp-11-9631-2011, 2011.

Wozniak, M. C. and Steiner, A. L.: A prognostic pollen emissions model for climate models (PECM1.0), Geosci. Model Dev., 10, 4105–4127, https://doi.org/10.5194/gmd-10-4105-2017, 2017.

Yuan, H., Dai, Y., Xiao, Z., Ji, D., and Shangguan, W.: Reprocessing the MODIS Leaf Area Index products for land surface and climate modelling, Remote Sens. Environ., 115, 1171–1187, https://doi.org/10.1016/j.rse.2011.01.001, 2011.

Zhang, L., Gong, S., Padro, J., and Barrie, L.: A size-segregated particle dry deposition scheme for an atmospheric aerosol module, Atmos. Environ., 35, 549–560, https://doi.org/10.1016/S1352-2310(00)00326-5, 2001.

Ziemba, L. D., Beyersdorf, A. J., Chen, G., Corr, C. A., Crumeyrolle, S. N., Diskin, G., Hudgins, C., Martin, R., Mikoviny, T., Moore, R., Shook, M., Thornhill, K. L., Winstead, E. L., Wisthaler, A., and Anderson, B. E.: Airborne observations of bioaerosol over the Southeast United States using a Wideband Integrated Bioaerosol Sensor, J. Geophys. Res.-Atmos., 121, 8506–8524, https://doi.org/10.1002/2015JD024669, 2016.

Zink, K., Pauling, A., Rotach, M. W., Vogel, H., Kaufmann, P., and Clot, B.: EMPOL 1.0: a new parameterization of pollen emission in numerical weather prediction models, Geosci. Model Dev., 6, 1961–1975, https://doi.org/10.5194/gmd-6-1961-2013, 2013.

Document History

Version	Author(s)	Date	Changes
1.0	Samuel Remy and Gunnar Lange	4/7/2025	Initial version

Internal Review History

Internal Reviewers	Date	Comments